Nanoscale Advances

Accepted Manuscript

This article can be cited before page numbers have been issued, to do this please use: X. Yang, J. Shu, Z. Zhou and H. Liang, *Nanoscale Adv.*, 2024, DOI: 10.1039/D4NA00292J.

ROYAL SOCIETY OF CHEMISTRY

rsc.li/nanoscale-advances

View Article Online
DOI: 10.1039/D4NA00292J

Declaration of interests

☒ The authors declare that they have no known competing financial interests or personal relationships that could have appeared to influence the work reported in this paper.

☐ The authors declare the following financial interests/personal relationships which may be considered as potential competing interests:

View Article Online
DOI: 10.1039/D4NA00292J

Polyimide as a biomedical material: advantages and applications

Junjie Shu [1], Zhongfu Zhou [2], Huaping Liang [1*] and Xia Yang [1*]

[1] Department of Wound Infection and Drug, State Key Laboratory of Trauma and Chemical Poisoning, Daping Hospital, Army Medical University (Third Military Medical University), Chongqing, China

[2] Inner Mongolia Key Laboratory of New Carbon Materials, Baotou, China

[*]Corresponding authors. E-mail addresses: 13638356728@163.com (H. Liang), oceanyx@126.com (X. Yang).

View Article Online
DOI: 10.1039/D4NA00292J

Abstract

As a class of polymers, polyimides (PIs) are characterized by strong covalent bonds, which have the advantages of high thermal weight, low weight, good electronic properties and superior mechanical properties. They have been successfully used in the fields of microelectronics, aerospace engineering, nanomaterials, lasers, energy storage and painting. Its biomedical application has attracted extensive attention, and it has been explored for its use as an implantable, detectable, and antibacterial material in recent years. This article summarizes the progress of PI in terms of three aspects: synthesis, properties, and application. First, the synthetic strategies for PI are summarized. Then, the properties of PI as a biological or medical material are analyzed. Finally, the applications of PI in electrodes, biosensors, drug delivery systems, bone tissue replacements, face masks or respirators, and antibacterial materials are introduced. The present review provides a comprehensive understanding of the newest progress of the PI, thereby providing a basis for developing new potentially promising materials for medical applications.

Keywords: polyimide; synthesis; characters; properties; medical application.

View Article Online
DOI: 10.1039/D4NA00292J

1. Introduction

After decades of research in materials science and tissue engineering, the capacity to create functional human tissue models for the whole repair of organ functions *in vivo* and *in vitro* is still challenging. A large number of materials and technologies have been constructed, investigated, and manufactured, but only a few have been successfully applied in the clinic. To achieve successful translation of medical materials into clinical practice, the ideal characteristics of these materials include the ability to mimic native organ structure and function, no toxicity, perfect integration into and interaction with tissues, and adaptation of the morphology and function of the organism, including sufficient vascular supply, no thrombus and active response to challenging environments such as cancer, inflammation, and infection[1]. Therefore, an increasing number of investigations focusing on medical materials have been designed due to some directional improvements that could rescue the functions of organs and tissues.

Currently, successful examples of applications of medical materials such as intraocular lenses[2], poly(4-methyl-1-pentene) (PMP) artificial lung membranes for extracorporeal membrane oxygenation (ECMO)[3], and filtration membranes for continuous renal replacement therapies (CRRTs)[4] have provided groundbreaking solutions to the choke points in related fields with the rapid development of medical devices, and the demands of some of these medical-related materials are considerable. For example, there are more than 7-20 million lens implant candidates annually worldwide[5]. The cost of ECMO therapy support for surviving adult patients diagnosed with acute respiratory distress syndrome is high, at approximately $98,784,116[6]. A total of 68% of 100,000 ECMO survivors are treated at more than 300 centers worldwide [6], and ECMO has been proven to be an effective approach for saving the lives of these patients. The global market demand for hemostatic material was valued at USD

View Article Online
DOI: 10.1039/D4NA00292J

20.8 billion in 2022 and is predicted to progressively increase at a compound annual growth rate of 5.4% from 2022 to 2027[7]. This situation worldwide encourages academics as well as the pharmaceutical and medical dressing or equipment industries to investigate more new products for the treatment of these diseases. However, in some cases, the properties of these materials cannot meet clinical expectations under complex pathological conditions *in vivo*. For example, artificial blood vessels that can be long-term implanted in the body without adverse reactions such as thrombosis caused by lower limb ischemia are lacking [8]. The oxidized cellulose-based commercial hemostatic material Surgicel® is highly effective in blocking small arterial bleeding and reducing intracranial hematoma in bleeding patients. However, the acidic microenvironment can potentially induce an inflammatory response, delaying the wound-healing process and damaging peripheral nerves[9]. How can we improve the functions and overcome the shortcomings of these materials? One effective way is to develop composite materials, which is a new hope for expanding the range of single biomaterial applications in the medical field. For example, chitosan combined with quaternary ammonium groups improved the antibacterial properties of this special material [10]. Another way is continuing to innovate the existing medical material and technology, and the materials become increasingly complicated and diversified; the performance of these newer medical materials could satisfy the demands with no additional adverse reactions.

Notably, numerous studies have shown that polyimide (PI) has excellent physical and chemical properties, including low weight, flame retardancy, high-temperature resistance, low-temperature tolerance, excellent mechanical properties, chemical solvent and radiation resistance, flexibility, and good dielectric properties [11]. It has been concluded that PI has been proven to be an important industry material for military armor, aerospace areas, radomes, liquid crystal alignments, microelectronics,

View Article Online
DOI: 10.1039/D4NA00292J

solar-to-electrochemical energy storage, photocatalysis, electrocatalysis applications,etc.[12]. PIs are now widely used as membranes for the insulation of solar cell base plates and motor slots, for separating membranes in permeation vaporization and ultrafiltration, for repairing enameled wire, for insulating fibres in high-temperature media and bulletproof and fireproof fabrics, for adhesives in high-temperature structural adhesives, for photoresists in color filter films, for microelectronics in dielectric layers and protective layers, for liquid crystal displays in orientation agent materials, for electro-optical materials in optical switch fields and composites in aviation and aerospace fields[13, 14]. Additionally, advanced healthcare PIs were designed to include puncture needle-type devices, artificial hip joints, microelectrode arrays for nerve stimulation[15], drug delivery[16, 17], biosensors[18], and other aspects of medical utilization[19, 20]. Therefore, several recent studies have described the design of PIs for medical material applications, including resins, powders, films, fibers, foams, and soluble PIs (Fig. 1). We aim to review the relevant literature on the synthesis and structural characteristics, properties, and application of PI as a medical material and its trends and outlook in the present review.

2. Synthesis of PI

PIs with cyclic aliphatic, hetero, chiral, fluorinated, carbazole, nonlinear optical, nanometer-sized and unsymmetrical structures are derived from noncoplanar monomers (kink, spiro, and cardo structures). PIs can be divided into aliphatic and aromatic polyimides according to their chemical composition. Aromatic PIs are commonly synthesized from the polycondensation of various monomers, including diamine and dianhydride, which are composed of a sequence of aromatic groups with imide linkages (-CO-N-CO-)[21]. PI fibers were initially carried out by Americans as early as the 1960s and then investigated by Japanese, Soviet, French, Austrian, and Chinese investigators [22].

View Article Online
DOI: 10.1039/D4NA00292J

2.1 Typical synthesis process

The typical synthesis process of PI involves the loading of crystalline benzoic acid (BA) (9.0 g) and phthalic anhydride (PA) (0.7287 g) into a glass reactor equipped with a heater, stirrer, and an inert gas inlet. With the gas in the reactor at 140°C, 3,4′-ODA (0.2803 g) was added to the mixture. The reaction mixture was stirred at 150°C for 2 h, accompanied by the slow addition of inert gas. Then, this hot liquid reaction mixture was transferred to a glass container and cooled to room temperature. Next, the solidified reaction mixture was extracted and washed repeatedly with acetone or diethyl ether to remove the excess BA. Finally, the reaction product of the polymer was filtered and dried under vacuum, and PI powder was obtained. One improved method reported that PI was also obtained in 99% yield within 1 h from a polyamic acid intermediate using the "beat and heat" method, which included solvent-free vibrational ball milling and a thermal treatment step[23]. After the PI powder was obtained, it was hot pressed at 300∽380℃ or from a 2% solution in chloroform to form PI films (Fig. 2A) [24]. This study presented a straightforward route to synthesize PI powders and films.

2.2 Dry- and wet-spinning methods

Some studies have reported that PI fibers are mostly synthesized by dry-spinning and wet-spinning methods. In the wet-spinning method, organic-soluble PI or polyamic acid (PAA) solutions are forced into a nonsolvent fluid to separate the fibres from the solvent. Then, the generated fibers are annealed under tension to remold the tensile strength and modulus. Compared with the wet-spinning method, organic solvents are evaporated directly from extruded PAA fibers at high temperatures, and a partial imidization reaction occurs in a mixture of hot gases during the dry-spinning process (Fig. 2B)[22]. The spinning speed is increased to improve the production of PI fibers by the dry-spinning process. The quality of PI fibers is better when using wet-spinning or dry-wet-spinning methods.

View Article Online
DOI: 10.1039/D4NA00292J

2.3 One-step and two-step processes

In addition, according to the main difference between spinning solutions and reaction mechanisms, two main strategies, defined as one-step and two-step processes, are also used to prepare PI fibers. In a one-step method, PI fibers are produced directly from highly boiling organic-soluble PI solutions at 180-220°C to undergo a rapid imidization reaction. In the two-step method, PAA solutions are obtained first after reacting dianhydride and diamine monomers in dipolar aprotic solvents and then converted into final PI fibers through thermal or chemical imidization (Fig. 2C)[25]. P-phenylenediamine (PDA) and 3,3',4,4′-biphenyltetra-carboxylic dianhydride (BPDA) are combined to obtain precursor fibers of PAA via a dry-jet wet-spinning process. Subsequently, the PAA fibers were heated from room temperature to 300, 350, and 400°C to form PI fibers, and the tensile modulus of the PI fibers was highly dependent on the heating rate[25]. In addition, PAA can also be obtained from the reaction of 4,4'-oxydianiline (4,4'-ODA) (3.97 g) and pyromellitic dianhydride (PMDA) (4.33 g) in 35 ml of N,N-dimethylformamide (DMF) by polycondensing with stirring for 8 h. The PAA solution was electrospun at 15 kV 15 cm from the needle to the collector and then subjected to thermal imidization (Fig. 2D)[26]. Finally, PI nanofibers were prepared.

2.4 Thermoplastic or thermosetting methods

According to their processing characteristics, PI fibers can also be classified as thermoplastic or thermosetting. The thermoplastic partially crystalline PI powder was distributed on continuous carbon fibers via electrostatic spraying, and further hot calendering and pressing were applied. The obtained carbon plastics lead to a rise in glass transition and thermal decomposition temperatures up to 590°C due to being composited with PI (Fig. 2E)[27]. The physical properties of thermosetting PI include a higher glass transition temperature and storage modulus and better shape fixity than thermoplastic PI due to low-density covalent crosslinking (Fig.

View Article Online
DOI: 10.1039/D4NA00292J

2F)[28]. Hyperbranched PI was prepared to modify bismaleimide (BMI) resin to achieve higher impact strength (Fig. 2G)[29]. Based on the use of chemical or physical crosslinking reactions, thermoplastic or thermosetting processes are chosen.

2.5 The modified synthesis process

Moreover, other investigations have investigated the imidization process, evaporation, chain orientation, crystallization, subprocesses of solvents, chemical conversion, and composition to improve the properties of PI materials [25]. The PIs synthesized from symmetric 4,4'-oxydianiline (4,4'-ODA) are amorphous and have a low glass transition temperature (Fig. 2H)[30]. The introduction of 2,4,5,7-tetraamino-1,8-dihydroxyanthracene-9,10-dione (4NADA) monomers in the polyimide chains can enhance the rigidity of the structure[31].

A new dianhydride, 10-oxo-9-phenyl-9-(trifluoromethyl)-9,10-dihydroanthracene-2,3,6,7-tetraacid dianhydride (3FPODA), was proven to be an ideal candidate monomer for enhancing the adhesive properties and glass transition temperatures (Tg) of colorless PI (Fig. 2I)[32]. One special flexible PI film obtained using a multicomponent copolymerization methodology from a fluoro-containing dianhydride, 4,4'-hexafluoroisopropylidene)diphthalic anhydride (6FDA), a rigid dianhydride, 3,3',4,4'-biphenyltetracarboxylic dianhydride (BPDA), and a fluoro-containing diamine,2,2´-bis(trifluoromethyl)-4,4'-bis[4- (4-amino-3-methyl)benzamide]biphenyl (MABTFMB), showed good optical properties and excellent thermal properties (Fig. 2J)[33].

It was concluded that the methods of PI synthesis are completely complicated. By changing the elements, the ratio of monomers, and the preparation method, hundreds of thousands of PIs with different characteristics can be obtained.

The application and popularization of PI could improve due to improvements in synthesis strategies and spinning technology.

View Article Online
DOI: 10.1039/D4NA00292J

3. Properties of PI as a biological/medical material

To be a biomedical polymer material, some basic characteristics need to be met. These include but are not limited to (1) being chemically inert, not due to contact with body fluids; (2) not causing inflammation or foreign body reactions to human tissues; (3) not causing cancer; (4) not clotting on the surface of the material, with antithrombotics; (5) long-term implantation in the body, with which the mechanical strength does not decrease; (6) being able to withstand the necessary cleaning and disinfection measures without degeneration; and (7) being easy to process into the required complex shape. It is worth mentioning that PI not only meets all the conditions of interest but also shows beneficial biological activity[34, 35]. The following characteristics are a list of the advantages of the PI used in the medical field.

3.1 Long-term stability

PI and PI matrix nanocomposites have attracted increasing attention for material applications due to their high thermal stability at high temperatures. The thermogravimetric degradation profiles of pure PI show that the initial decomposition of PI occurs in the temperature range of 200-400°C because of the release of chemically bound water and evaporation of the solvent. The PI matrix achieved 40% mass loss at 500-630°C (Fig. 3A)[36]. The high-temperature resistance of the PI composite films was modified by integration with mica nanosheets (Fig. 3B)[37]. In a 20-month *in vitro* study, three commercially available PIs, U-Varnish-S (UBE, Japan), Durimim 7510 (FUJIFILM, Japan), and PI2611 (HD MicroSystems, USA), were immersed in phosphate-buffered saline (PBS, pH=7.4) at special temperatures. After 20 months, the experimental PI did not undergo mass loss at 37°C (normal human body temperature) or 60°C (upper limit temperature for accelerated lifetime testing) in PBS, and the fracture mechanical properties, such as fracture energy, did not change (Fig. 3C-E)[38]. A new thin-film PI-based electrode array was stimulated by

View Article Online
DOI: 10.1039/D4NA00292J

electricity and then immersed in PBS at body temperature (37±3°C) for 29 d. The electrical characteristics were evaluated by cyclic voltammetry (CV), electrochemical impedance spectroscopy (EIS), and voltage transients (VT). The results showed the stable electrode material of the PI electrode array [39]. PBS obviously does not fully represent the complex environment in the body. Studies on the long-term biological stability of PI *in vivo* have also been reported. After being implanted in animals, the PI electrode can work stably for months or even a year[40-42]. Cross-sectional imaging using focused ion beam scanning electron microscopy (FIB-SEM) revealed well-adhered layers of the metallic electrode and PI, and no aging phenomena, such as delamination or cracking, occurred (Fig. 3 F-H)[40]. Similar results were obtained after implantation of the PI material into rabbit eyes for 6 months. Light microscopy and SEM revealed that the PI materials did not obviously degrade (Fig. 3I)[15]. These results suggest that PI could be an ideal implanted material that maintains the dual stability of the PI itself and the implant environment.

3.2 Multiple Construction Process

PI is formulated in various forms, such as films, fibers, resins, foams, flexible electronic substrates, gas separation membranes, proton exchange membranes, and soluble PI, with different physical and chemical properties. Different forms of PI can be further modified to obtain thousands of properties according to different synthesis and processing processes, which gives PI great potential to be designed and manufactured with variable functionalities according to different requirements. For example, stiff forms of PI can be made into puncture needle-type devices (e.g., transverse intrafascicular multichannel electrodes)[43], while neural electrodes attached to the cerebral cortex require flexible PI[44]. Different curing temperatures[45] and surface modifications[46] can change the hydrophobicity and roughness of PI materials. A smooth surface is suitable for the cardiovascular system and helps to reduce the risk of

View Article Online
DOI: 10.1039/D4NA00292J

thrombosis [47], while a rough surface facilitates fibroblast and osteoblast attachment [48]. Changes in surface morphology can also strengthen the differentiation of mesenchymal stem cells into adipogenic and osteogenic lineages *in vitro* [49], which can be applied in the field of wound repair. In addition, porous PI can be used as a drug delivery system. Different drugs can be loaded, and the release rate becomes controllable due to the different pore sizes of PI [50]. Excitingly, the features of multiple construction processes of PI provide an effective method to perform numerous chemical modifications that could be advanced to overcome the shortcomings of present materials.

3.3 Biocompatibility

Materials scientists recognize that "biocompatibility" is a characteristic of the material-biological host response system, not the property of the material itself in a specific application[51]. Cytotoxicity testing is an essential aspect of evaluating biocompatibility. Richardson et al. showed for the first time that PI has no cytotoxic effects on mouse fibroblast (Swiss-3T3) cells, similar to polytetrafluoroethylene (PTFE) and polydimethylsiloxane (PDMSO) (usually used as hydrophobic substrates for plaster drugs)[52]. After that, the cytotoxicity of PI to L929 mouse fibroblasts[53], human retinal pigment cells (Fig. 4A)[15], human epithelial cells (adherent HeLa)[54], human cerebromicrovascular endothelial cells (hCMECs) (Fig. 4B)[55] and human dermal fibroblasts[56] was tested. Some of these studies claim to follow ISO standards strictly. Other studies have used 3-(4,5)-Dimethylthiahiazo (-z-y1)-3,5-diphenyltetrazoliumromide (MTT) assays, lactic dehydrogenase-based toxicology assays, calcein-AM, and ethidium bromide-based live/dead assays. All *in vitro* experiments suggested that PI has low/noncytotoxic effects.

Although investigators widely use cytotoxicity testing and are the only biocompatibility experiments for many biomaterial-related studies, it is obvious that *in vitro* studies of single cell lines and simple environments

View Article Online
DOI: 10.1039/D4NA00292J

are far from able to explain biocompatibility problems *in vivo*. As the understanding of biocompatibility has deepened, an increasing number of studies have begun to explore the hemocompatibility (i.e., does not cause hemolysis or coagulation) of PIs (Fig. 4C, 4D)[57], genotoxicity[58], irritation[59], and host response[60]. New thin-film PI electrodes were also tested in biocompatibility studies, including acute systemic toxicity, irritation, pyrogenicity, sensitization, immune system response, and a prolonged 28-d subdural implant *in vivo* (Fig. 4E)[61]. In these studies, neither the PI nor implants with the PI as the main material were found to cause severe negative effects *in vitro* or *in vivo*. Fortunately, new thin-film PI electrodes were permitted by the US FDA for clinical trials [510(k) K192764], making it possible to use these electrodes as the first subdural electrode to develop rapidly from studies to the clinic, indicating that more long-term *in vivo* studies of PI are needed to prove its biocompatibility. However, a five-year safety study of minimally invasive glaucoma surgery showed that patients implanted with PI materials (Micro-Stent) experienced more endothelial cell loss over time than patients who underwent only standard cataract surgery (loss 20.4% vs. 10.1%) (Fig. 4F)[62]. This suggests that more long-term *in vivo* studies of PI need to be performed due to the special PI materials with low cytotoxicity.

4. Medical applications of polyimides

As one of the high-performance classes of polymers, an increasing number of studies have focused on broadening the applications of PI.

The superior high- or low-temperature tolerance, chemical solvent and radiation resistance, flexibility, dielectric properties, biocompatibility, long-term stability and multiple construction process properties of PI have made its use possible from industry to medicine. The medical applications of PIs are listed and summarized in Table 1.

4.1 PI electrodes in the nervous system

Electrodes that function as signal collectors and transmitters are mainly

View Article Online
DOI: 10.1039/D4NA00292J

used in the study, diagnosis, and treatment of diseases. They have attracted much attention as important components of neuron-computer interfaces in recent years. For example, intracranial nerve electrodes collect raw physiological signals and are the most important part of the entire signal-processing process[63]. The integrated electrode itself needs to be long-lasting and stable while minimizing adverse effects on the organism to collect the clearest and most stable signal (Fig. 5A)[40]. The choice of substrate material is crucial. In this regard, the combination of the two properties of "flexibility" and "small cross-sectional area" seems to be particularly effective [42, 64]. PI, as an excellent material for meeting this requirement, has high potential to serve as an electrode in neural applications due to its biocompatibility[64], electrochemical inertity[42], electrical conductivity, and long-term stability (Fig. 5B)[40]. An increasing number of studies have investigated PIs with different backbones used for integrated microelectrodes (Fig. 5C)[42].

Microelectrodes fabricated from fully aromatic PIs show superior performance for the electrochemical monitoring of dopamine and provide evidence for the early diagnosis of neurological disorders[65]. A flexible PI is also used as a substrate to develop epidural electrocorticography electrodes, which can monitor various neurodegenerative diseases[66]. One PI-based flexible electrode can record electrocorticography signals in multiple regions with minimal invasiveness of the brain (Fig. 5D)[67]. Moreover, a brain intracranial electroencephalogram microdisplay engineered by the PI as a substrate to measure brain neuronal activity successfully identifies the boundaries of normal versus pathological brain regions and displays changes in near real-time on the surface of the brain in the surgical field [68]. The nanofabricated PI-based microelectrode for high-resolution mouse electroencephalography is a competent tool for recording large-scale brain activity and accommodating the ability to distinguish the neural correlates of certain brain waves in conjunction

View Article Online
DOI: 10.1039/D4NA00292J

with special behavior[69]. One special electrode that combines PI with prototype carbon records the signaling of the neural local field with an equal or better signal-to-noise ratio and almost completely removes image artifacts at magnetic fields of strength up to 9.4 T and is potentially useful for electrophysiology and magnetic resonance imaging for neurological diseases[70]. In addition, PI electrodes are also applied for recording output signals in human nerves in the robotic arms of amputees[71]. The photosensitive PI microelectrode arrays (epiretinal bio-MEAs) lying on the visual cortex in the eyes of rabbits successfully recorded the response to electrical stimuli (Fig. 5E)[15].

Furthermore, electrical neuron stimulation also provides promising methods for treating and diagnosing chronic neurological diseases, such as epilepsy. New thin-film PI electrodes for use in clinical trials for surgical evaluation of patients with drug-resistant epilepsy have been announced only by the FDA[61]. A microlight-emitting diode array with a flexible PI film used as a chronic photostimulation unit and a whole-cortex electrocorticographic electrode used as a recording unit were implanted into the cerebral cortex of common marmosets for 4 months. This device gradually increased neural responses after photostimulation for ~8 weeks [72] and has potential applications for epilepsy treatment. In peripheral nerves, PI-based implantable flexible microelectrode arrays (MEAs), which provide nerve stimulation and recording on the surface of long-term denervated muscles, can reduce the atrophy of denervated muscle while retaining more acetylcholine receptors[73]. One transverse intrafascicular multichannel electrode was transversally implanted into the rat sciatic nerve and the median human nerve to interface with the peripheral nerve (Fig. 5F-G)[43]. The PI-based MEAs can be further used for the stimulation of remaining retinal neurons in patients with degenerated photoreceptors [15, 74].

However, mice implanted with PI-based microelectrodes on free muscle

View Article Online
DOI: 10.1039/D4NA00292J

flap grafts and subjected to electrical stimulation for 6 weeks exhibited an increased inflammatory response, myopathy, and partial necrosis [75]. These studies suggested that the multiple functionalities of PI electrodes provide exciting opportunities for fundamental neuroscience studies, as well as for stimulation-based neural therapies, but future work should carefully investigate the optimal electrode material, graft, and stimulated phase.

4.2 PI in biosensors

Implantable or noninvasive biosensors used as real-time monitors are powerful devices for diagnosing and predicting disease and maintaining human health by monitoring and providing continuous or regular biometric signals. Like neural electrodes, biosensors (which transmit physical or chemical signals) often use PI as a sensor substrate because of its good biocompatibility, hemocompatibility, and other properties. PIs were fabricated as thin, flexible, and implantable neuroprobes with aptamer-field-effect transistor biosensors for neurochemical signaling monitoring [18]. PI has been applied in interventional procedures, such as real-time monitoring of cerebral aneurysm hemodynamics (Fig. 6A)[76]. The microphone array integrated into the PI can be used to qualify hemodialysis vascular access dysfunction (location and degree of stenosis) (Fig. 6B)[77]. A novel biosensor that manufactured an array of 64 hybrid cantilevers with a PI substrate detected drug-induced adverse effects at early stages, such as depolarization and Torsade de Points, in cardiomyocytes (Fig. 6C)[16]. One miniature fiber optic pressure sensor fabricated with PI, which is tiny enough to be implanted into rodent discs without changing the structure or changing the intradiscal pressure, was first successfully applied for rodent intradiscal pressure measurements (Fig. 6D)[78]. Furthermore, a multichannel temperature sensor fabricated from a flexible PI film can wrap around a dental implant abutment wing and then send real-time warning signals before failure of the implant (Fig. 6E)[79].

View Article Online
DOI: 10.1039/D4NA00292J

It has also been reported that biosensors made with PI as a substrate have excellent abilities for trace-level or specific detection of the concentrations of some hormones, glucose, and gases produced by the body or others. One flexible biosensor was prepared by direct synthesis of molybdenum disulphide (MoS2) on a PI substrate, which can be sensitively used for the determination of endocrinopathy by measuring endocrine-related hormones, such as parathyroid hormone (PTH), triiodothyronine (T3), and thyroxine (T4), in clinical patient sera[80]. Ultrasensitive sensor arrays on PI substrates can be used for multiplexed and simultaneous electrochemical detection of cardiac damage markers, cardiac troponin-I (cTnI) and cardiac troponin-T (cTnT), in human serum[81]. A porous PI film sensor combined with grafted MgO-templated carbon can be applied to sensitively measure acetaldehyde gas released by human skin, even at low concentrations[82]. A special human sweat-based wearable glucose sensor microfabricated with reduced graphene oxide on a flexible PI substrate and integrated chitosan-glucose oxidase composites exhibited sensitive, rapid, and stable response performance for detecting glucose from human sweat (Fig. 6F)[83].

A PI-based film bulk acoustic resonator (PI-FBAR) humidity sensor operating for the first time was utilized for detecting human respiratory rates in real-time *in vitro* (Fig. 6G)[84]. One biosensor made of highly porous graphitic carbon electrodes fabricated with commercial PI tape offers rapid, low-cost, time-saving, selective, and sensitive electrochemical detection for point-of-care analysis of cytokines such as IL6 [85]. In addition, neuronal cells were generated on biosensors printed with few-layer graphene ink onto Kapton PI to evaluate the electrophysiology and electrical signaling of Parkinson's disease *in vitro*[86]. Lin R. et al. reported that an ultrathin PI microsensor array can be integrated into a puncture needle for early detection of small volumes of blood extravasation (Fig. 6H)[87]. As a small spring constant of PI, PI/Si/SiO2-based piezoresistive

microcantilever biosensors were developed to sensitively and precisely detect aflatoxin B1 in various foods and other biomolecules[88]. Sensors integrated with PI as substrates have the potential to satisfy the need for innovative examination or analytic platforms owing to their high throughput, sensitivity, biocompatibility, and simplified data analysis.

4.3 PI in drug delivery systems

Drug modifications, microenvironmental modifications, and drug delivery systems are the three core paradigms of drug delivery technology. Drug delivery systems can build an interface between the drug and its microenvironment, adjusting and optimizing the activity of the drug[17]. Polymers generated by the PI form the basis of many drug delivery systems for multiple functions, such as controlled release and targeted release. Lumen drug-loaded PI tubing with micro-holes in the tube wall has been made into a diffusion-controlled reservoir-type implantable device[89]. The device was implanted subcutaneously in mice and achieved stable drug release for several months (Fig. 7A)[90]. Microneedles are an advanced transdermal drug delivery system. The introduction of PI can increase the mechanical strength of microneedle arrays of carbon nanotubes, providing skin penetration with a smaller insertion force (Fig. 7B)[91, 92]. In interventional surgery, PI microcatheter-oriented cephalad in the internal carotid artery allows for reproducible delivery of drugs to the ipsilateral cerebral hemisphere (Fig. 7C)[93]. The drugs gentamicin, dexamethasone, and lidocaine can be delivered to the tympanic chamber through PI microtubing at the round window membrane into the cochlea[94]. One special covalent organic framework (COF) synthesized from PI loaded with ibuprofen exhibited high drug loading and well-controlled release (Fig. 7D)[50]. PI-based transdermal skin patches have been applied for the controlled release of ondansetron after chemotherapy[95]. Similarly, PI and reduced graphene oxide composite transdermal patches have also been used in insulin delivery (Fig. 7E)[96]. Additionally, flexible PI probes

View Article Online
DOI: 10.1039/D4NA00292J

can be used for highly localized drug delivery and can be applied to study electrical and chemical information exchange and communication between cells both *in vitro* and *in vivo* (Fig. 7F)[97].

The PI-based drug delivery device is a promising way to establish precise, high-volume loading, good release control, and safety for drug delivery applications.

4.4 PI in bone tissue replacements and artificial muscles

It is universally acknowledged that metallic materials are the most commonly used implants for load-bearing bone repair[98]. However, metallic implants with a high elastic modulus have stress-shielding effects that result in bone resorption and bone atrophy, leading to loosening or failure of the implants[99]. Due to their relative inertness, superior mechanical strength, elastic modulus, bioactivity, and biocompatibility, PI biomaterials are attractive materials that could be applied to bone tissue and joint replacement candidates for replacing traditional cartilage materials. The biological inertness of PI indicates a reduced inflammatory response. However, PI, a bioinert material used as a bone substitute, cannot induce a cell response, bone development and repair or osteointegration, which are important foundations for eventual bone healing[100].

To resolve this problem, the surface bioactive properties of PI for potential bone substitutes have improved [38]. Kaewmanee et al. used concentrated sulfuric acid to treat PI, creating microporous surface phenotypes on the materials. At the same time, flower-like molybdenum disulphide submicron-spheres added to sulfuric acid in advance are attached to the microporous surface of PI, resulting in the final PI-molybdenum disulphide composites, which exhibit good osteogenic and antibacterial functions (Fig. 8A-F)[101]. Moreover, the microporous PI coating with 15 w% tantalum oxide submicron-particles resulted in greater bioactivity, and cellular responses (such as proliferation, adhesion, and

alkaline phosphatase activity) were induced by bone marrow stromal cells from rats (Fig. 8G-L)[102]. In particular, Zhang et al. reported that 40 W% nanolaponite ceramic fabricated with PI through melt processing could increase the bioactivity of PI as an implantable material for bone repair. The greater amount of apatite deposited on this composite material indicates good bioactivity; it exhibited outstanding proliferation, cell adhesion, and alkaline phosphatase activity in rat bone mesenchymal stem cells *in vitro* and remarkably induced osteogenesis and osseointegration in male beagle dogs *in vivo* (Fig. 8M-O)[103].

In addition to bone substitutes, PI is also used in the design of artificial muscles. Ling et al. added a corrugated grid-like PI scaffold inside a muscle prosthesis to simulate the undulated perimysial collagen fibers surrounding the myocardium, making the contraction of the muscle prosthesis direction-dependent and more in line with physiological conditions[104].

Overall, these findings show that this bioengineering approach involving PI provides promising strategies for fabricating biomimetic bone substitutes for bone repair and muscle reconstruction.

4.5 PI in face masks or respirators

The traditional N95 mask provides 85% protection for sub300 nm particles. Unfortunately, it cannot meet the demand to protect against pathogens such as the COVID-19 virus, which has a diameter of 65-125 nm[105]. Since the outbreak of COVID-19 across the globe, antipathogen mask design and decontamination methods involving N95/N99 masks have been preferentially studied and developed[106]. By utilizing the hydrophobicity and low pore size (down to 5 nm) of PI nanofiber membranes, investigators have focused on the outstanding filter performance of PI materials. PI electrospun fibers with embedded metal-organic frameworks are made to mask and perform well at filtering volatile organic compounds represented by formaldehyde[107]. Polyimide and

View Article Online
DOI: 10.1039/D4NA00292J

polyethersulfone solutions have been used in electrospinning to develop nanofiber membranes with excellent filtration efficiency for particulate matter, excellent filter quality for nano-aerosols, excellent interception ratios for bacteria and viruses (above 99%), and nontoxic effects on cells [108]. In addition, PI has also been introduced into the design of photothermal self-purification masks. With the help of plasmonics, the surface temperature of the respirators increases to more than 80°C within 1 min after exposure to sunlight, enabling convenient inactivation and reuse of microorganisms [109]. However, in the study of Ghatak et al., PI-nylon did not show a superior triboelectric ability to latex rubber[110]. Crucially, the low price of raw materials makes the mass generation of PI-based masks feasible. This finding suggested that the filtration efficiency of the PI mask against bacteria, viruses, volatile organic compounds, and polluted air needs to be confirmed before use.

4.6 PI as an antibacterial material

The reported experimental results showed that the antibacterial ability includes antibacterial adhesion, antibacterial biofilm formation, inhibition of bacterial growth under coculture, and accelerated wound healing of infection.

It is worth noting that some studies exploring the antimicrobial effect of PI composites have only tested the antimicrobial ability of the composite as a whole and have not tested PI alone, where PI is considered a hydrophobic matrix/carrier and the antimicrobial activity defaults to its non-PI component[101]. It has also been found that the PI used in composite materials exhibits low antibacterial activity[102, 111, 112]. PIs modified with a concentrated sulfuric acid suspension containing 15% tantalum oxide submicron-particles (named PIST15) exhibited improved antibacterial properties[102]. Topographically and chemically modified commercial PI films (Kapton, American) improved the antibacterial properties of these materials, decreasing bacterial *Pseudomonas aeruginosa* (*P. aeruginosa*)

adhesion and inhibiting bacterial growth but not triggering cell death in the attached bacteria[113].

Recently, there have been successful studies in which only PI was used to make antibacterial medical catheters and dressings (here, PI is not a matrix of composite antimicrobial materials). Lee et al. developed a surface-modified medical PI catheter that forms an antifouling layer, as its surface is modified with hydrophilic amino acids. *In vitro* experiments have shown that the adhesion of bacteria, fibrinogen, and albumin on the surface of the duct decreases significantly, which is highly important for the prevention of catheter-associated infections[114]. Polymer films based on 2-methacryloyloxyethyl phosphorylcholine-modified hyperbranched PI synthesized directly significantly reduced the number of adhesive bacteria and improved the antibacterial properties in *in vitro* experiments[115]. The CuFe2O4@SiO2-PI nanoparticles exhibited good biocompatibility with HEK293T cells and antibacterial properties against *P. aeruginosa, Escherichia coli* (*E. coli*), and *Staphylococcus aureus* (*S. aureus*)[116]. In our group, wound dressings made of PI fibers showed significant antimicrobial effects on methicillin-resistant *S. aureus* (MRSA) and *E. coli* in *in vitro* experiments. It was found that the PI fibers directly damaged the cell walls of both bacteria. *In vivo*, PI dressings effectively improved local infection of smeared wounds in mice, inhibited the bacterial load, reduced infiltrating macrophages, and accelerated the healing of pathogen-infected wounds[34]. We used other forms of PI materials with similar original materials, but different polymerization reactions were used to investigate the antibacterial properties of these materials (Fig. 9). However, specific PI fibers exhibit significant antibacterial effects *in vitro*[34].

Studies have shown that PI materials have excellent antibacterial properties and possess many other advantages, such as biocompatibility, long life, and reusability. These successful examples may indicate that PI

View Article Online
DOI: 10.1039/D4NA00292J

antimicrobial materials are expected to be applied in the clinic in the near future.

5. Trends and Outlook

Recent progress in controlled polymerization has led to the development of diverse, complex composites for various applications. PI is considered to be one of the polymer materials with the best overall performance and has been broadly investigated due to its unique features and application in advanced materials. However, apart from the great amount of progress summarized in the present review, some challenges still need to be met for PI technology in either theoretical or practical aspects in medical areas in the future for translating PI materials into practical applications.

Methods to control the appearance, characteristics, and function of PIs for medical applications have been developed. Synthesizing composite materials and changing the inherent properties of PIs are possible ways to improve the application range of PIs. With current technology, it is easy to change some properties of PI, such as morphology, hardness, thermal conductivity, and insulation. However, with the rapid development of the medical field of polymers, both *in vitro* and *in vivo*, more PIs with better performance will be developed. For example, improving the electrical feasibility of insulation PIs has attracted increasing attention. Conductive materials offer advantages, such as complex conductive biomaterial-based wound dressings with conductivity similar to that of human skin, which can significantly enhance wound healing.

As the complexity of electrodes increases, the challenges associated with their manufacture and clinical applications also increase. Overcoming the damage to tissue by electrode implantation, inevitable glial scarring, inflammation, and neuronal loss accompanying all implantable neurotechnologies within months remains the greatest demand. Furthermore, to protect the functional neuronal circuitry near electrodes, a great deal of effort has been invested in improving the biocompatibility of

View Article Online
DOI: 10.1039/D4NA00292J

neural probes.

As sensors, these challenges include detecting analyte concentrations at ultralow levels (down to parts per billion or nanomolar levels), coping with complex sample matrices containing numerous interfering species, addressing issues related to differentiating isomers and structural analogs and managing intricate, multidimensional data sets. Advanced artificial intelligence techniques, including machine learning, could help boost the performance of these kinds of sensors for medical applications, nanotoxicology, neural prostheses, wireless technology, smart agriculture, environmental monitoring, and advanced medical manufacturing technologies.

There is an urgent need for modified industrial and medical masks that provide additional air filtration and deactivate pathogens using various technologies. Polymers with inherent micropores in the fiber matrix perform better in filtration, among which filter membranes based on PI fibers featuring macro, meso-, and micropores and good filtration efficiency have been designed. Investigators are also trying to use the electrical energy generated by the self-friction of masks to directly kill pathogens or provide electricity for sensors and antipathogen devices. Researchers have investigated the cytotoxicity of PI, particularly the fate of PI when it interacts with mammalian cells or is implanted *in vivo*. Comprehending this area will lead to the development of next-generation PI medical materials that confirm safety guarantees for clinical applications.

6. Conclusion

The demands for biomaterials and medical devices have attracted attention recently worldwide. The safety and performance of these materials should be a priority when considering the conditions and the environment that would most benefit patients in repairing organ functions. PI is one of the most important high-performance and advanced polymers. In this review,

View Article Online
DOI: 10.1039/D4NA00292J

we introduce the chemical composition, structural features, spinning solutions, and reaction mechanism and then summarize the properties of PI and its practical applications. It was suggested that different forms of PI, including power, films, fibers, resins, foams, and soluble PI, have different characteristics and applications. PIs have been studied and manufactured as neural electrodes, sensors, drug delivery systems, tissue replacements, masks, antimicrobial catheters, and antimicrobial dressings in healthcare. Overall, this review will form a design guideline for future PI materials/devices and help investigators overcome the obstacles to further functional improvement for PI applications in the medical field.

Conflicts of interest

There are no conflicts of interest to declare.

Acknowledgments

This research was supported by the Specialized Program (NO. 2022-JCJQ-ZD-224-12) and the Chongqing Talent Project (NO. Cstc2021ycjh-bgzxm0340). We want to thank Prof. Zheng Chunfu for helpful discussions and for polishing the grammatical presentation of this manuscript.

Table 1. Summary of the medical applications of PI.

Applications	Devices	Functions
Neural Electrodes	Electrocorticography (ECoG) arrays	Dopamine monitoring[65]，high-Performance neural recordings[61, 66, 67, 69], pathological brain regions identification[68] , chronic stimulation [72]
	Peripheral electrodes	Epiretinal stimulation[15]， motor nerve stimulation[43]，denervated muscles stimulation[73], afferent nerve simulation[71]
	Depth probes	Brain-computer interface[40], chronic stimulation and monitoring[42]
Biosensor	Vessel-related sensors	Aneurysm monitoring[76], stenosis monitoring[77], extravasation detection[87]

	In vitro sensors	Cells' electrical signaling sensing[86], electrochemical detection[85]
	Implant sensors	Intradiscal pressure measurement[78], dental implant detection[79]
Drug Delivery Systems	PI tubes	Controlled-release subcutaneously[89]， inner ear drug delivery[94]，intracranial drug delivery[93]
	Microneedles	Painless subcutaneous drug delivery[91, 92]
	transdermal patches	Electrothermal and photothermal triggered drug release[95, 96]
	PI-COF	High drug loading and well-controlled release[50]
Tissue Replacements	Artificial bones	Osteogenesis and osseointegration inducing[101, 103, 111]
	Artificial muscle	Simulating perimysial collagen fibers[104]
Respirators	Medical masks	Self-friction generating electric energy[117], photothermal self-purification[109]
Antibacterial Material	Medical catheter	Anti-biofilm formation[114],
	Anticoagulant membrane	Antibacterial adhesion[115]
	Dressing	Bacteria killing and healing promoting[34]

View Article Online
DOI: 10.1039/D4NA00292J

References

1. L. De Laporte and F. Kiessling, *Advanced Healthcare Materials*, 2023, **12**, 2301637.
2. M. Wilczynski, O. Wilczynska and W. Omulecki, *Klin Oczna*, 2009, **111**, 21-25.
3. Y. Wang, Y. Liu, Q. Han, H. Lin and F. Liu, *J Memb Sci*, 2022, **649**, 120359.
4. D. Y. Fuhrman, E. K. Stenson, I. Alhamoud, R. Alobaidi, G. Bottari, S. Fernandez, F. Guzzi, T. Haga, A. Kaddourah, E. Marinari, T. H. Mohamed, C. J. Morgan, T. Mottes, T. M. Neumayr, N. J. Ollberding, V. Raggi, Z. Ricci, E. See, N. L. Stanski, H. Zang, E. Zangla, K. M. Gist and W.-R. Investigators, *JAMA Netw Open*, 2024, **7**, e240243.
5. E. H. Leung, A. Gibbons and D. D. Koch, *Ophthalmology*, 2020, **127**, 859-865.
6. A. Garcia and N. D. Giraldo, *Biomedica*, 2022, **42**, 707-716.
7. A. Shariati, S. M. Hosseini, Z. Chegini, A. Seifalian and M. R. Arabestani, *Biomed Pharmacother*, 2023, **158**, 114184.
8. Y. Tamura and T. Abe, *Clin Case Rep*, 2023, **11**, e7276.
9. E. Spaziani, A. Di Filippo, P. Francioni, M. Spaziani, A. De Cesare and M. Picchio, *Acta Chir Belg*, 2018, **118**, 48-51.
10. L. Wang, M. Xin, M. Li, T. Zhang, Y. Pang and Y. Mao, *Carbohydr Res*, 2024, **538**, 109078.
11. S. Ma, S. Wang, S. Jin, Y. Wang, J. Yao, X. Zhao and C. Chen, *Polymer*, 2020, **210**.
12. Y. Zhang, Z. Huang, B. Ruan, X. Zhang, T. Jiang, N. Ma and F. C. Tsai, *Macromol Rapid Commun*, 2020, **41**, e2000402.
13. K. Choi, A. Droudian, R. M. Wyss, K. P. Schlichting and H. G. Park, *Sci Adv*, 2018, **4**, eaau0476.
14. H. S. Bi, X. X. Zhi, P. H. Wu, Y. Zhang, L. Wu, Y. Y. Tan, Y. J. Jia, J. G. Liu and X. M. Zhang, *Polymers (Basel)*, 2020, **12**.
15. X. Jiang, X. Sui, Y. Lu, Y. Yan, C. Zhou, L. Li, Q. Ren and X. Chai, *J Neuroeng Rehabil*, 2013, **10**, 48.
16. D. S. Kim, Y. J. Jeong, A. Shanmugasundaram, N. E. Oyunbaatar, J. Park, E. S. Kim, B. K. Lee and D. W. Lee, *Biosens Bioelectron*, 2021, **190**, 113380.
17. A. M. Vargason, A. C. Anselmo and S. Mitragotri, *Nat Biomed Eng*, 2021, **5**, 951-967.
18. C. Zhao, T. Man, Y. Cao, P. S. Weiss, H. G. Monbouquette and A. M. Andrews, *ACS Sens*, 2022, **7**, 3644-3653.

19. X. Dong, L. Chen, J. Liu, S. Haller, Y. Wang and Y. Xia, *Sci Adv*, 2016, **2**, e1501038.
20. M. Kanno, H. Kawakami, S. Nagaoka and S. Kubota, *J Biomed Mater Res*, 2002, **60**, 53-60.
21. S. A. Tharakan and S. Muthusamy, *RSC Adv*, 2021, **11**, 16645-16660.
22. M. Zhang, H. Niu and D. Wu, *Macromol Rapid Commun*, 2018, **39**, e1800141.
23. T. Rensch, S. Fabig, S. Gratz and L. Borchardt, *ChemSusChem*, 2022, **15**, e202101975.
24. A. E. Soldatova, R. N. Shamsutdinova, T. V. Plisko, K. S. Burts, A. Y. Tsegelskaya, D. A. Khanin, K. Z. Monakhova, T. S. Kurkin, A. V. Bildyukevich and A. A. Kuznetsov, *Materials (Basel)*, 2022, **15**.
25. W. Yang, F. Liu, H. Chen, X. Dai, W. Liu, X. Qiu and X. Ji, *Polymers (Basel)*, 2020, **12**.
26. Z. Chang, X. Sun, Z. Liao, Q. Liu and J. Han, *Polymers (Basel)*, 2022, **14**.
27. G. Vaganov, M. Simonova, M. Romasheva, A. Didenko, E. Popova, E. Ivan'kova, A. Kamalov, V. Elokhovskiy, V. Vaganov, A. Filippov and V. Yudin, *Polymers (Basel)*, 2023, **15**.
28. X. Xiao, D. Kong, X. Qiu, W. Zhang, Y. Liu, S. Zhang, F. Zhang, Y. Hu and J. Leng, *Sci Rep*, 2015, **5**, 14137.
29. L. Yu, Y. Yu, J. Shi, X. Zhang, F. Gao, C. Li, Z. Yang and J. Zhao, *Polymers (Basel)*, 2022, **14**.
30. Y. Zi, D. Pei, J. Wang, S. Qi, G. Tian and D. Wu, *Polymers (Basel)*, 2021, **13**.
31. B. Liu, Y. Zhou, L. Dong, Q. Lu and X. Xu, *iScience*, 2022, **25**, 105451.
32. Y. Wang, X. Liu, J. Shen, J. Zhao and G. Tu, *Polymers (Basel)*, 2022, **14**.
33. X. Ren, H. Wang, X. Du, H. Qi, Z. Pan, X. Wang, S. Dai, C. Yang and J. Liu, *Materials (Basel)*, 2022, **15**.
34. X. Yang, W. Ma, H. Lin, S. Ao, H. Liu, H. Zhang, W. Tang, H. Xiao, F. Wang, J. Zhu, D. Liu, S. Lin, Y. Zhang, Z. Zhou, C. Chen and H. Liang, *Nanoscale Adv*, 2022, **4**, 3043-3053.
35. I. Antanaviciute, L. Simatonis, O. Ulcinas, A. Gadeikyte, B. Abakeviciene, S. Tamulevicius, V. Mikalayeva, V. A. Skeberdis, E. Stankevicius and T. Tamulevicius, *J Tissue Eng Regen Med*, 2018, **12**, e760-e773.
36. C. Akinyi and J. O. Iroh, *Polymers (Basel)*, 2023, **15**.
37. X. F. Pan, B. Wu, H. L. Gao, S. M. Chen, Y. Zhu, L. Zhou, H. Wu and S. H. Yu, *Adv Mater*, 2022, **34**, e2105299.
38. B. Rubehn and T. Stieglitz, *Biomaterials*, 2010, **31**, 3449-3458.
39. S. Ong, A. Kullmann, S. Mertens, D. Rosa and C. A. Diaz-Botia, *Micromachines (Basel)*, 2022, **13**.
40. C. Bohler, M. Vomero, M. Soula, M. Voroslakos, M. Porto Cruz, R. Liljemalm, G. Buzsaki, T. Stieglitz and M. Asplund, *Adv Sci (Weinh)*, 2023, **10**, e2207576.
41. A. Kilias, Y. T. Lee, U. P. Froriep, C. Sielaff, D. Moser, T. Holzhammer, U. Egert, W. Fang, O. Paul and P. Ruther, *J Neural Eng*, 2021, **18**.

View Article Online
DOI: 10.1039/D4NA00292J

42. M. Vomero, F. Ciarpella, E. Zucchini, M. Kirsch, L. Fadiga, T. Stieglitz and M. Asplund, *Biomaterials*, 2022, **281**, 121372.
43. T. Boretius, J. Badia, A. Pascual-Font, M. Schuettler, X. Navarro, K. Yoshida and T. Stieglitz, *Biosens Bioelectron*, 2010, **26**, 62-69.
44. E. Otte, A. Vlachos and M. Asplund, *Cell Tissue Res*, 2022, **387**, 461-477.
45. Y. Sun, S. P. Lacour, R. A. Brooks, N. Rushton, J. Fawcett and R. E. Cameron, *J Biomed Mater Res A*, 2009, **90**, 648-655.
46. W. Ma, Y. Ding, M. Zhang, S. Gao, Y. Li, C. Huang and G. Fu, *J Hazard Mater*, 2020, **384**, 121476.
47. Y. Liang, M. Ernst, F. Brings, D. Kireev, V. Maybeck, A. Offenhausser and D. Mayer, *Adv Healthc Mater*, 2018, **7**, e1800304.
48. M. Voisin, M. Ball, C. O'Connell and R. Sherlock, *Nanomedicine*, 2010, **6**, 35-43.
49. G. Abagnale, M. Steger, V. H. Nguyen, N. Hersch, A. Sechi, S. Joussen, B. Denecke, R. Merkel, B. Hoffmann, A. Dreser, U. Schnakenberg, A. Gillner and W. Wagner, *Biomaterials*, 2015, **61**, 316.
50. Q. Fang, J. Wang, S. Gu, R. B. Kaspar, Z. Zhuang, J. Zheng, H. Guo, S. Qiu and Y. Yan, *J Am Chem Soc*, 2015, **137**, 8352-8355.
51. M. Kowalczuk, *Polymers (Basel)*, 2020, **12**.
52. R. R. Richardson, Jr., J. A. Miller and W. M. Reichert, *Biomaterials*, 1993, **14**, 627-635.
53. D. Serbezeanu, T. Vlad-Bubulac, D. Rusu, G. G. Pircalabioru, I. Samoila, S. Dinescu and M. Aflori, *Materials (Basel)*, 2019, **12**.
54. S. Nagaoka, K. Ashiba and H. Kawakami, *Artif Organs*, 2002, **26**, 670-675.
55. P. Starr, C. M. Agrawal and S. Bailey, *J Biomed Mater Res A*, 2016, **104**, 406-412.
56. A. M. Feldweg, D. S. Friend, J. S. Zhou, Y. Kanaoka, M. Daheshia, L. Li, K. F. Austen and H. R. Katz, *Eur J Immunol*, 2003, **33**, 2262-2268.
57. L. I. Buruiana, A. I. Barzic, I. Stoica and C. Hulubei, *Journal of Polymer Research*, 2016, **23**, 217.
58. E. Efsa Panel on Food Contact Materials, A. Processing, V. Silano, J. M. Barat Baviera, C. Bolognesi, A. Chesson, P. S. Cocconcelli, R. Crebelli, D. M. Gott, K. Grob, C. Lambre, E. Lampi, M. Mengelers, A. Mortensen, I. L. Steffensen, C. Tlustos, H. Van Loveren, L. Vernis, H. Zorn, L. Castle, E. Di Consiglio, R. Franz, N. Hellwig, M. R. Milana, K. Pfaff, K. Volk and G. Riviere, *EFSA J*, 2020, **18**, e06183.
59. C. Y. Lin, W. S. Lou, J. C. Chen, K. Y. Weng, M. C. Shih, Y. W. Hung, Z. Y. Chen and M. C. Wang, *Micromachines (Basel)*, 2020, **11**.
60. L. J. Shen, Y. Q. Chen, D. Cheng, C. Zhang, L. Jiang, M. Hong and Q. Y. Kang, *Curr Eye Res*, 2016, **41**, 79-87.
61. A. Kullmann, D. Kridner, S. Mertens, M. Christianson, D. Rosa and C. A. Diaz-Botia, *Front Neurosci*, 2022, **16**, 876877.
62. J. H. Lass, B. A. Benetz, J. He, C. Hamilton, M. Von Tress, J. Dickerson and S. Lane, *Am J Ophthalmol*, 2019, **208**, 211-218.

63. X. Strakosas, H. Biesmans, T. Abrahamsson, K. Hellman, M. S. Ejneby, M. J. Donahue, P. Ekstrom, F. Ek, M. Savvakis, M. Hjort, D. Bliman, M. Linares, C. Lindholm, E. Stavrinidou, J. Y. Gerasimov, D. T. Simon, R. Olsson and M. Berggren, *Science*, 2023, **379**, 795-802.
64. Z. Zhao, H. Zhu, X. Li, L. Sun, F. He, J. E. Chung, D. F. Liu, L. Frank, L. Luan and C. Xie, *Nat Biomed Eng*, 2023, **7**, 520-532.
65. K. H. Nam, M. Abdulhafez, E. Castagnola, G. N. Tomaraei, X. T. Cui and M. Bedewy, *Carbon N Y*, 2022, **188**, 209-219.
66. M. E. E. Alahi, Y. Liu, S. Khademi, A. Nag, H. Wang, T. Wu and S. C. Mukhopadhyay, *Biosensors (Basel)*, 2022, **12**.
67. U. J. Jeong, J. Lee, N. Chou, K. Kim, H. Shin, U. Chae, H. Y. Yu and I. J. Cho, *Lab Chip*, 2021, **21**, 2383-2397.
68. Y. Tchoe, T. Wu, H. S. U, D. M. Roth, D. Kim, J. Lee, D. R. Cleary, P. Pizarro, K. J. Tonsfeldt, K. Lee, P. C. Chen, A. M. Bourhis, I. Galton, B. Coughlin, J. C. Yang, A. C. Paulk, E. Halgren, S. S. Cash and S. A. Dayeh, *bioRxiv*, 2023, DOI: 10.1101/2023.07.19.549735.
69. M. Lee, D. Kim, H. S. Shin, H. G. Sung and J. H. Choi, *J Vis Exp*, 2011, DOI: 10.3791/2562.
70. C. E. Cruttenden, J. M. Taylor, S. Hu, Y. Zhang, X. H. Zhu, W. Chen and R. Rajamani, *Biomed Phys Eng Express*, 2017, **4**.
71. P. M. Rossini, S. Micera, A. Benvenuto, J. Carpaneto, G. Cavallo, L. Citi, C. Cipriani, L. Denaro, V. Denaro, G. Di Pino, F. Ferreri, E. Guglielmelli, K. P. Hoffmann, S. Raspopovic, J. Rigosa, L. Rossini, M. Tombini and P. Dario, *Clin Neurophysiol*, 2010, **121**, 777-783.
72. M. Komatsu, E. Sugano, H. Tomita and N. Fujii, *Front Neurosci*, 2017, **11**, 514.
73. M. McAvoy, J. K. Tsosie, K. N. Vyas, O. F. Khan, K. Sadtler, R. Langer and D. G. Anderson, *Theranostics*, 2019, **9**, 7099-7107.
74. S. H. Bae, J. H. Che, J. M. Seo, J. Jeong, E. T. Kim, S. W. Lee, K. I. Koo, G. J. Suaning, N. H. Lovell, D. I. Cho, S. J. Kim and H. Chung, *Invest Ophthalmol Vis Sci*, 2012, **53**, 2653-2657.
75. S. Srinivasan, K. Vyas, M. McAvoy, P. Calvaresi, O. F. Khan, R. Langer, D. G. Anderson and H. Herr, *Front Neurol*, 2019, **10**, 252.
76. R. Herbert, S. Mishra, H. R. Lim, H. Yoo and W. H. Yeo, *Adv Sci (Weinh)*, 2019, **6**, 1901034.
77. B. Panda, S. Mandal and S. J. A. Majerus, *IEEE Trans Biomed Circuits Syst*, 2019, **13**, 1494-1505.
78. S. Nesson, M. Yu, X. Zhang and A. H. Hsieh, *J Biomed Opt*, 2008, **13**, 044040.
79. J. J. Kim, G. R. Stafford, C. Beauchamp and S. A. Kim, *Sensors (Basel)*, 2020, **20**.
80. H. U. Kim, H. Y. Kim, H. Seok, V. Kanade, H. Yoo, K. Y. Park, J. H. Lee, M. H. Lee and T. Kim, *Anal Chem*, 2020, **92**, 6327-6333.
81. N. Radha Shanmugam, S. Muthukumar, S. Chaudhry, J. Anguiano and S. Prasad, *Biosens Bioelectron*, 2017, **89**, 764-772.

82. I. Shitanda, T. Oshimoto, N. Loew, M. Motosuke, H. Watanabe, T. Mikawa and M. Itagaki, *Biosens Bioelectron*, 2023, **238**, 115555.
83. X. Xuan, H. S. Yoon and J. Y. Park, *Biosens Bioelectron*, 2018, **109**, 75-82.
84. Y. Zhu, P. Xia, J. Liu, Z. Fang, L. Du and Z. Zhao, *Micromachines (Basel)*, 2022, **13**.
85. P. S. Tan, E. Vaughan, J. Islam, N. Burke, D. Iacopino and J. B. Tierney, *Nanomaterials (Basel)*, 2021, **11**.
86. J. Guo, A. E. Niaraki Asli, K. R. Williams, P. L. Lai, X. Wang, R. Montazami and N. N. Hashemi, *Biosensors (Basel)*, 2019, **9**.
87. R. Lin, Y. Jin, R. R. Li, C. Jiang, J. Ping, C. J. Charles, Y. L. Kong and J. S. Ho, *Biosens Bioelectron*, 2022, **216**, 114651.
88. Y. Tian, Y. Liu, Y. Wang, J. Xu and X. Yu, *Sensors (Basel)*, 2021, **21**.
89. Z. J. Wu, Z. Luo, A. Rastogi, S. Stavchansky, P. D. Bowman and P. S. Ho, *Biomed Microdevices*, 2011, **13**, 485-491.
90. A. Rastogi, P. D. Bowman and S. Stavchansky, *Drug Deliv Transl Res*, 2012, **2**, 106-111.
91. N. Unver, S. Odabas, G. B. Demirel and O. T. Gul, *J Mater Chem B*, 2022, **10**, 8419-8431.
92. B. J. Lyon, A. I. Aria and M. Gharib, *Biomed Microdevices*, 2014, **16**, 879-886.
93. A. Santillan, D. G. Rubin, C. P. Foley, D. Sondhi, R. G. Crystal, Y. P. Gobin and D. J. Ballon, *J Neurosci Methods*, 2014, **222**, 106-110.
94. D. A. Borkholder, X. Zhu and R. D. Frisina, *J Control Release*, 2014, **174**, 171-176.
95. F. Teodorescu, G. Queniat, C. Foulon, M. Lecoeur, A. Barras, S. Boulahneche, M. S. Medjram, T. Hubert, A. Abderrahmani, R. Boukherroub and S. Szunerits, *J Control Release*, 2017, **245**, 137-146.
96. Q. Pagneux, R. Ye, L. Chengnan, A. Barras, N. Hennuyer, B. Staels, D. Caina, J. I. A. Osses, A. Abderrahmani, V. Plaisance, V. Pawlowski, R. Boukherroub, S. Melinte and S. Szunerits, *Nanoscale Horiz*, 2020, **5**, 663-670.
97. S. Metz, A. Bertsch, D. Bertrand and P. Renaud, *Biosens Bioelectron*, 2004, **19**, 1309-1318.
98. Y. Hu, Y. Wang, Q. Feng, T. Chen, Z. Hao, S. Zhang, L. Cai, X. Guo and J. Li, *Biomater Sci*, 2023, **11**, 3486-3501.
99. F. S. L. Bobbert, K. Lietaert, A. A. Eftekhari, B. Pouran, S. M. Ahmadi, H. Weinans and A. A. Zadpoor, *Acta Biomater*, 2017, **53**, 572-584.
100. A. J. T. Teo, A. Mishra, I. Park, Y. J. Kim, W. T. Park and Y. J. Yoon, *ACS Biomater Sci Eng*, 2016, **2**, 454-472.
101. R. Kaewmanee, F. Wang, Y. Pan, S. Mei, J. Meesane, F. Li, Z. Wu and J. Wei, *Biomater Sci*, 2022, **10**, 4243-4256.
102. S. Asadullah, S. Mei, K. Yang, X. Hu, F. Wang, B. Yu, Z. Wu and J. Wei, *J Mech Behav Biomed Mater*, 2021, **124**, 104800.

103. Y. Zhang, W. Jiang, S. Yuan, Q. Zhao, Z. Liu and W. Yu, *Int J Nanomedicine*, 2020, **15**, 9389-9405.
104. Y. Ling, W. Pang, J. Liu, M. Page, Y. Xu, G. Zhao, D. Stalla, J. Xie, Y. Zhang and Z. Yan, *Nat Commun*, 2022, **13**, 524.
105. N. El-Atab, N. Qaiser, H. Badghaish, S. F. Shaikh and M. M. Hussain, *ACS Nano*, 2020, **14**, 7659-7665.
106. M. Loeb, A. Bartholomew, M. Hashmi, W. Tarhuni, M. Hassany, I. Youngster, R. Somayaji, O. Larios, J. Kim, B. Missaghi, J. V. Vayalumkal, D. Mertz, Z. Chagla, M. Cividino, K. Ali, S. Mansour, L. A. Castellucci, C. Frenette, L. Parkes, M. Downing, M. Muller, V. Glavin, J. Newton, R. Hookoom, J. A. Leis, J. Kinross, S. Smith, S. Borhan, P. Singh, E. Pullenayegum and J. Conly, *Ann Intern Med*, 2022, **175**, 1629-1638.
107. F. Topuz, M. A. Abdulhamid, R. Hardian, T. Holtzl and G. Szekely, *J Hazard Mater*, 2022, **424**, 127347.
108. H. W. Chen, Y. L. Kuo, C. H. Chen, C. S. Chiou, W. T. Chen and Y. H. Lai, *Process Saf Environ Prot*, 2022, **167**, 695-707.
109. H. Zhong, Z. Zhu, P. You, J. Lin, C. F. Cheung, V. L. Lu, F. Yan, C. Y. Chan and G. Li, *ACS Nano*, 2020, **14**, 8846-8854.
110. B. Ghatak, S. Banerjee, S. B. Ali, R. Bandyopadhyay, N. Das, D. Mandal and B. Tudu, *Nano Energy*, 2021, **79**, 105387.
111. R. Kaewmanee, F. Wang, S. Mei, Y. Pan, B. Yu, Z. Wu, J. Meesane and J. Wei, *J Mater Chem B*, 2022, **10**, 5058-5070.
112. W. Ma, Y. Li, M. Zhang, S. Gao, J. Cui, C. Huang and G. Fu, *ACS Appl Mater Interfaces*, 2020, **12**, 34999-35010.
113. E. A. Cuello, L. E. Mulko, C. A. Barbero, D. F. Acevedo and E. I. Yslas, *Colloids Surf B Biointerfaces*, 2020, **188**, 110801.
114. D. U. Lee, D. W. Kim, S. Y. Lee, D. Y. Choi, S. Y. Choi, K. S. Moon, M. Y. Shon and M. J. Moon, *Colloids Surf B Biointerfaces*, 2022, **211**, 112314.
115. Q. Li, J. Li, G. Liao and Z. Xu, *J Mater Sci Mater Med*, 2018, **29**, 126.
116. R. Eivazzadeh-Keihan, Z. Sadat, A. Mohammadi, H. Aghamirza Moghim Aliabadi, A. Kashtiaray, A. Maleki and M. Mahdavi, *Sci Rep*, 2023, **13**, 9598.
117. M. Mariello, A. Qualtieri, G. Mele and M. De Vittorio, *ACS Appl Mater Interfaces*, 2021, **13**, 20606-20621.
118. T. K. Nguyen, M. Barton, A. Ashok, T. A. Truong, S. Yadav, M. Leitch, T. V. Nguyen, N. Kashaninejad, T. Dinh, L. Hold, Y. Yamauchi, N. T. Nguyen and H. P. Phan, *Proc Natl Acad Sci U S A*, 2022, **119**, e2203287119.

View Article Online
DOI: 10.1039/D4NA00292J

Figure legends

Fig. 1. Different forms of PI for different applications. PIs were prepared as fibers, films, foams, resins, electronic substrates, and liquids for analysis in different applications.

Fig. 2. Schematic representations of the synthesis of PI.

(A) Synthesis of aromatic polyimides based on unsymmetrical diamine 3,4'-ODA and various tetracarboxylic acid dianhydrides. Reproduced with permission[24]. Copyright 2022, MDPI. **(B)** Preparation of HSHMPI fibers through an integrated continuous wet-spinning method. Reproduced with permission [22]. Copyright 2018, WILEY-VCH. **(C)** Synthesis of a BPDA-PDA polyimide. Reproduced with permission [25]. Copyright 2020, MDPI. **(D)** The electrospinning process. Reproduced with permission [26]. Copyright 2022, MDPI. **(E)** Synthesis of polyimide R-BAPBs with different molecular weights. Reproduced with permission [27]. Copyright 2023, MDPI. **(F)** Synthesis of a BPADA-ODA PI. Reproduced with permission [28]. Copyright 2015, Nature Publishing Group. **(G)** Synthesis of bismaleimide resin modified with hyperbranched polyimide. Reproduced with permission [29]. Copyright 2022, MDPI. **(H)** Synthesis of a 6FDA/ODPA-ODA polyimide. Reproduced with permission[30]. Copyright 2021, MDPI. **(I)** The preparation of 3FPODA and synthesis of copolymerized polyimide. Reproduced with permission [32]. Copyright 2022, MDPI. **(J)** Synthesis of an organosoluble Fluoro-containing polyimide. Reproduced with permission [33]. Copyright 2022, MDPI.

Fig. 3. Stability tests for PI. (A) TGA thermograms for neat polyimide, graphene, and Cloisite 30B clay in a nitrogen atmosphere at a heating rate of 30°C/min. Reproduced with permission [36]. Copyright 2021, MDPI. **(B)** The tensile strength and Young's modulus of a PI-Mica film changed little after AO, UV, and high-temperature exposure. Reproduced with permission [37]. Copyright 2013, WILEY-VCH.

(C~E) The mass loss curve (C) and stress-strain curve (D, E) of PI stored in PBS showed that PI was stable in PBS at body temperature and even at

60°C. Reproduced with permission [38]. Copyright 2010, Elsevier. **(F~H)** Electrochemical impedance spectroscopy (F) and long-term imaging (G) of a PI probe implanted in the mouse cortex for 180 d. SEM image showing the overall intact probe and no signs of delamination or corrosion (H). Reproduced with permission [40]. Copyright 2023, WILEY-VCH. SEM of a microelectrode six months after implantation in rabbit eyes without damage to the surface or accumulation of tissue matter. Reproduced with permission [15]. Copyright 2013, Springer Nature.

Fig. 4. Biocompatibility tests for PI. (A) Rabbit retina layer six months after PI electrode implantation (upper) and control retina implantation (lower). Reproduced with permission [15]. Copyright 2013, Springer Nature. (B) Images of endothelial cells subjected to direct contact cytotoxicity microscopy. (a) Untreated control. (b) Methanol-treated positive control. (c) HDPE, negative material control. (d) Latex, positive material control. (e) PI. Reproduced with permission [55]. Copyright 2013, WILEY-VCH. **(C, D)** Hemocompatibility tests. The spreading of blood proteins (C), red blood cells, and platelets (D) over the surface of the poly(EPICLON-PPD) and Kapton (PI) films. Reproduced with permission [57]. Copyright 2016, Springer Nature. **(E)** The immune system responses to a PI electrode (a~d) implanted for 28 days in the sheep brain were minimal compared with those to the negative control material (e~h). These effects were evaluated via the accumulation of immune system cells, necrosis, neovascularization, fibrosis, and astrocytosis/fatty infiltration. Reproduced with permission[61]. Copyright 2022, Aura Kullmann. **(F)** Long-term safety study. PI material (CyPass) implantation increases endothelial cell loss over time in patients with cataracts. Reproduced with permission [62]. Copyright 2019, Elsevier.

Fig. 5. PI electrodes in the nervous system. (A) Schematic illustration of flexible nanomembranes wrapped around a sciatic nerve for long-term application of electrical stimuli and sensing. Reproduced with permission

[118]. Copyright 2022, PNAS. **(B)** Thin-film intracortical multilayer array probe, which is robust and flexible. Reproduced with permission [40]. Copyright 2023, WILEY-VCH. **(C)** 3D representation of depth probes within the brain cortex of a rat. Reproduced with permission [42]. Copyright 2022, Elsevier. **(D)** Subdural electrocorticography (ECoG) electrode arrays were positioned through a small window through the skull of the rat's brain. Reproduced with permission [67]. Copyright 2021, Royal Society of Chemistry. **(E)** A stimulating thin-film microelectrode array was implanted on the surface of a rabbit retina. Reproduced with permission [15]. Copyright 2013, Springer Nature. **(F, G)** The rat sciatic nerve (F) and the median human nerve (G) were transversally implanted with a transverse intrafascicular multichannel electrode (TIME) device. Reproduced with permission[43]. Copyright 2010, Elsevier.

Fig. 6. Different applications of PI-based biosensors.

(A) Implantable batteryless biosensor for real-time monitoring of cerebral aneurysm hemodynamics. Reproduced with permission [76]. Copyright 2019, WILEY-VCH. **(B)** Flexible sensor array for dialysis vascular access monitoring (recording and processing blood flow sounds to determine stenosis risk). Reproduced with permission [77]. Copyright 2019, MDPI. **(C)** Integrated strain sensing platform for high-throughput drug toxicity screening. Reproduced with permission[16]. Copyright 2021, Elsevier. **(D)** Miniature pressure sensor for the intradiscal pressure measurements. Reproduced with permission [78]. Copyright 2008, SPIE **(E)** A temperature sensor adheres around an abutment wing of the dental implant platform. Reproduced with permission [79]. Copyright 2020, MDPI. **(F)** Wearable sweat-based glucose biosensor. Reproduced with permission[83]. Copyright 2018, Elsevier. **(G)** Film bulk acoustic resonator humidity sensor. Reproduced with permission [84]. Copyright 2022, MDPI. **(H)** Microsensor array mounted on a 1.25 mm diameter needle for early detection of

View Article Online
DOI: 10.1039/D4NA00292J

extravasation in intravenous therapy. Reproduced with permission [87]. Copyright 2022, Elsevier.

Fig. 7. PIs in drug delivery systems. (A) Perforated PI tube for subcutaneous implantation. Reproduced with permission [90]. Copyright 2012, Springer US. **(B)** Hollow MN array for transdermal drug delivery. Reproduced with permission [91]. Copyright 2022, Royal Society of Chemistry. **(C)** PI microcatheters for intra-arterial delivery. Reproduced with permission [93]. Copyright 2013, Elsevier. **(D)** Structural representations of 3D porous PI covalent organic frameworks. Reproduced with permission [50]. Copyright 2020, ACS. **(E)** Electrothermal patches with PI substrates. Reproduced with permission [96]. Copyright 2020, Royal Society of Chemistry. **(F)** Illustration of an implantable, flexible PI probe with microelectrodes and microfluidic channels. Reproduced with permission[97]. Copyright 2004, Elsevier.

Fig. 8. SME images of different polyimide-based composites for bone replacement. (A-C) Flower-like molybdenum disulfide (fMD)-PI composites with 0%, 5 wt% and 10 wt% fMD contents. **(D-F)** A-C under different magnifications. Reproduced with permission[101]. Copyright 2022, Royal Society of Chemistry. **(G-I)** Tantalum oxide (vTO)–PI composites (PISTs) with 0%, 10%, and 15% vTO contents. **(J-L)** G-I under different magnifications. Reproduced with permission[102]. Copyright 2021, Elsevier. **(M-O)** Nanolaponite ceramic (LC)-PI composites (LPCs) with 0%, 20 wt% and 40 wt% LC content. **(P-R)** M-O under different magnifications. Reproduced with permission [103]. Copyright 2020, DOVE.

Fig. 9. Different types of PIs were synthesized to analyze their antibacterial properties. The different forms of PI were prepared as films, patches, fibers, fabrics, and gauze.

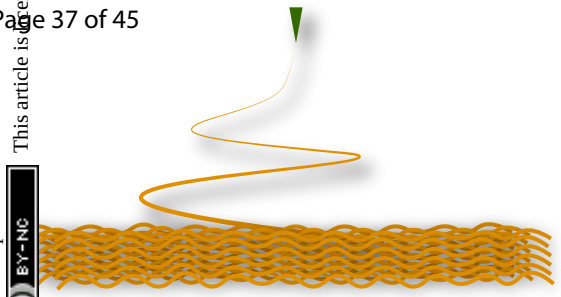

Electrospun Fiber

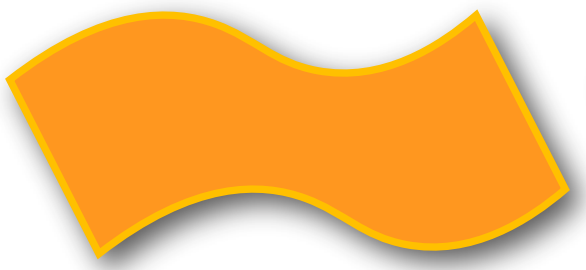

Film

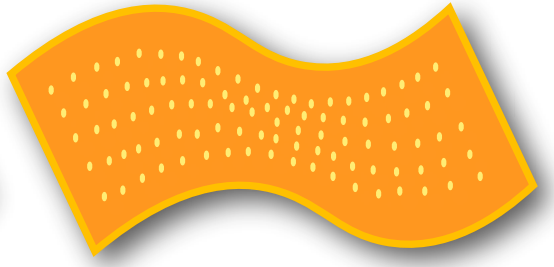

Porous Film

Foam

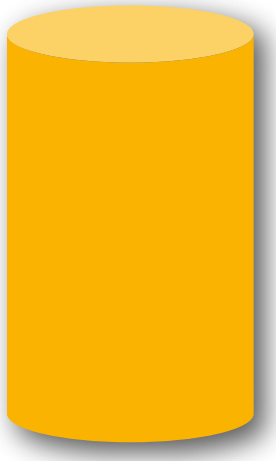

Smooth Resin

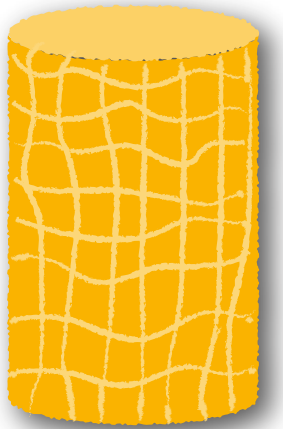

Rough Resin

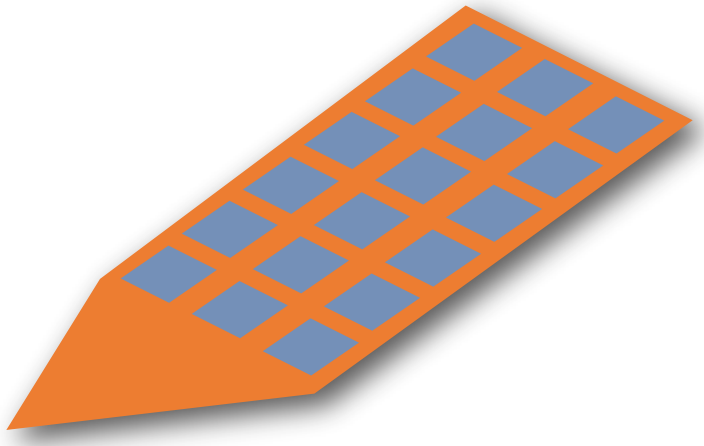

Flexible Electronic Substrate

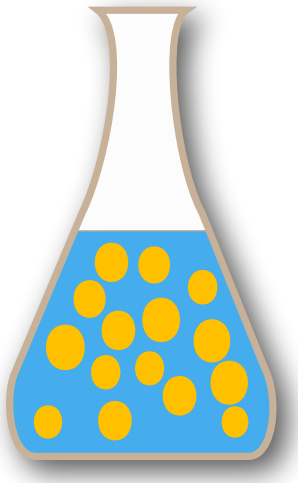

Soluble PI

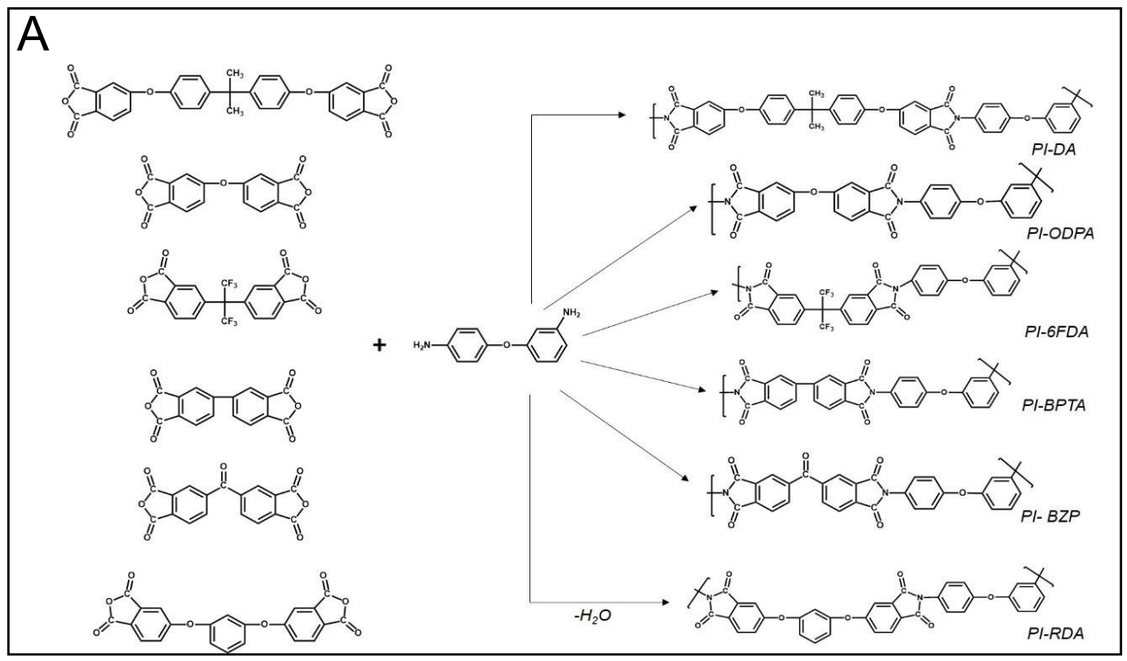

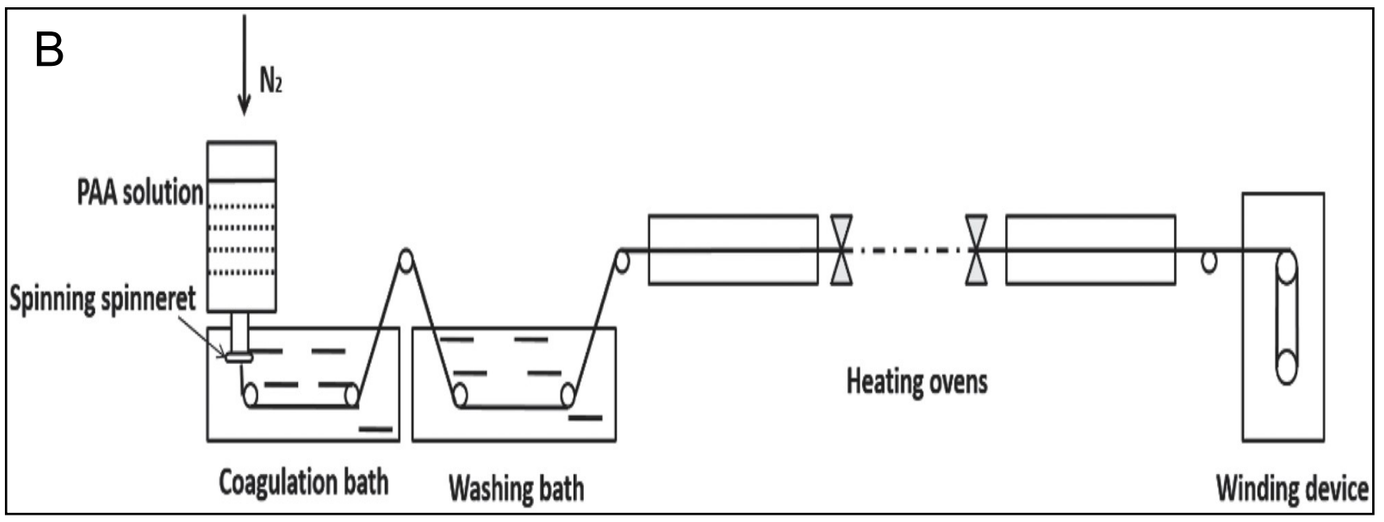

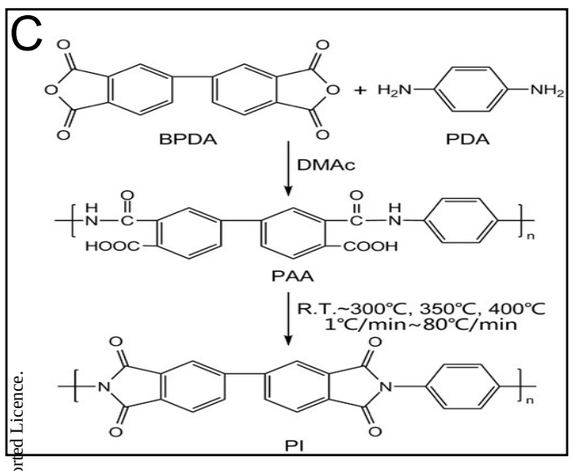

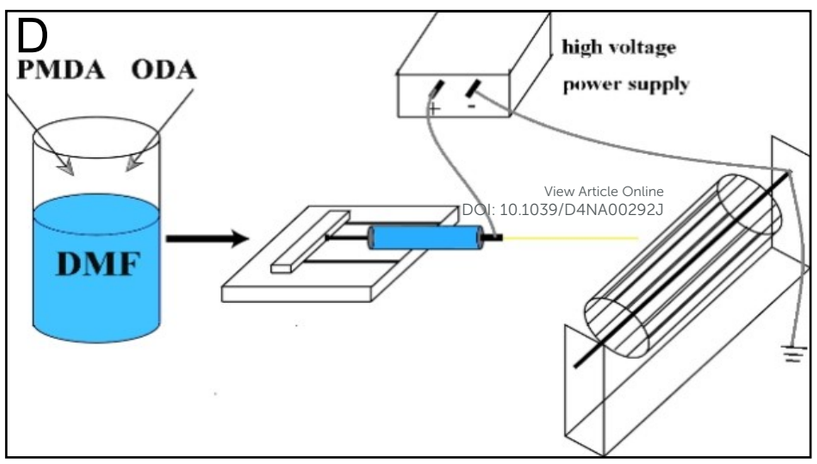

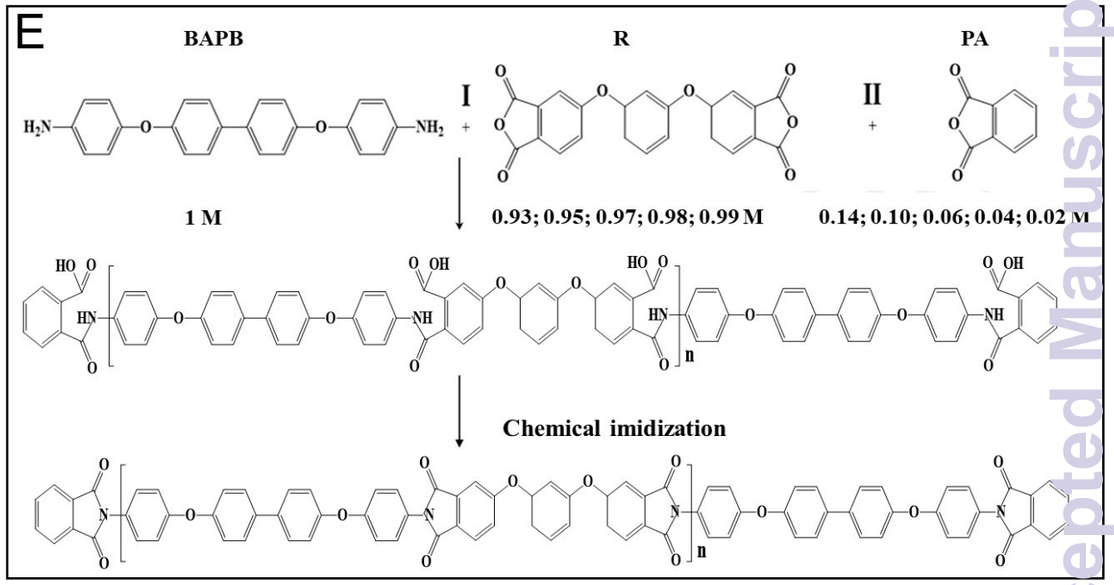

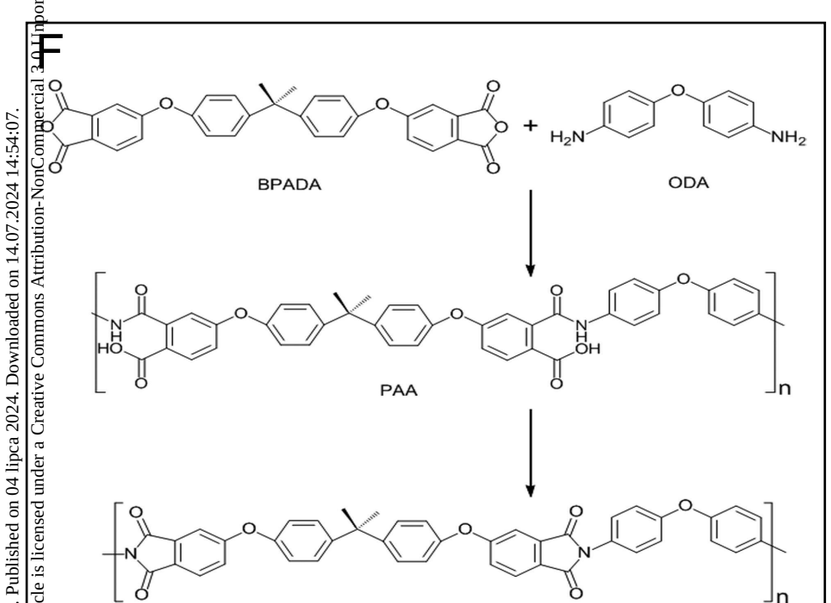

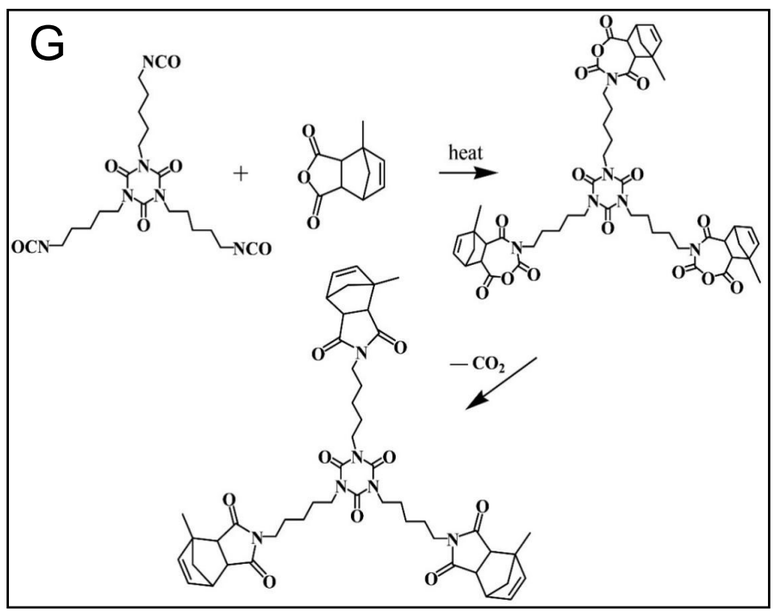

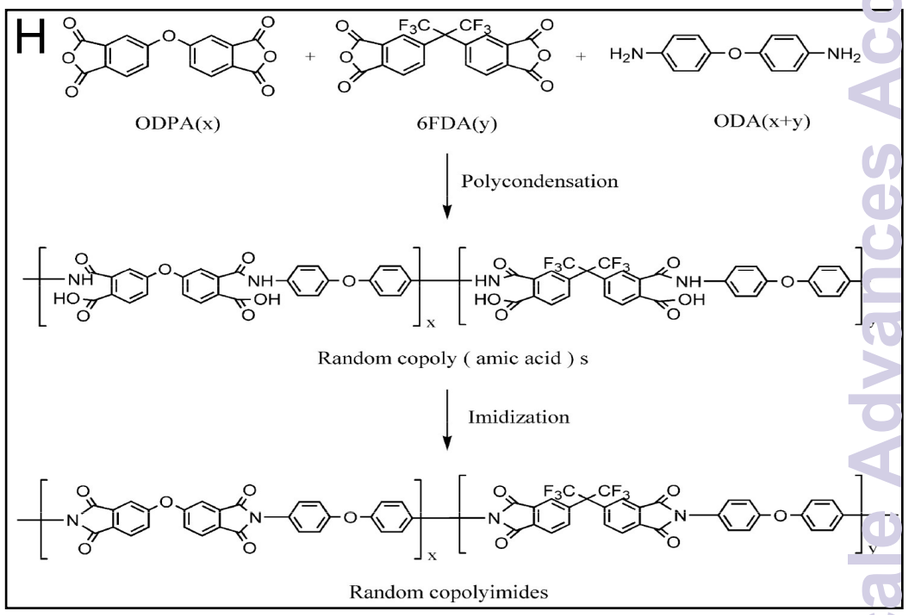

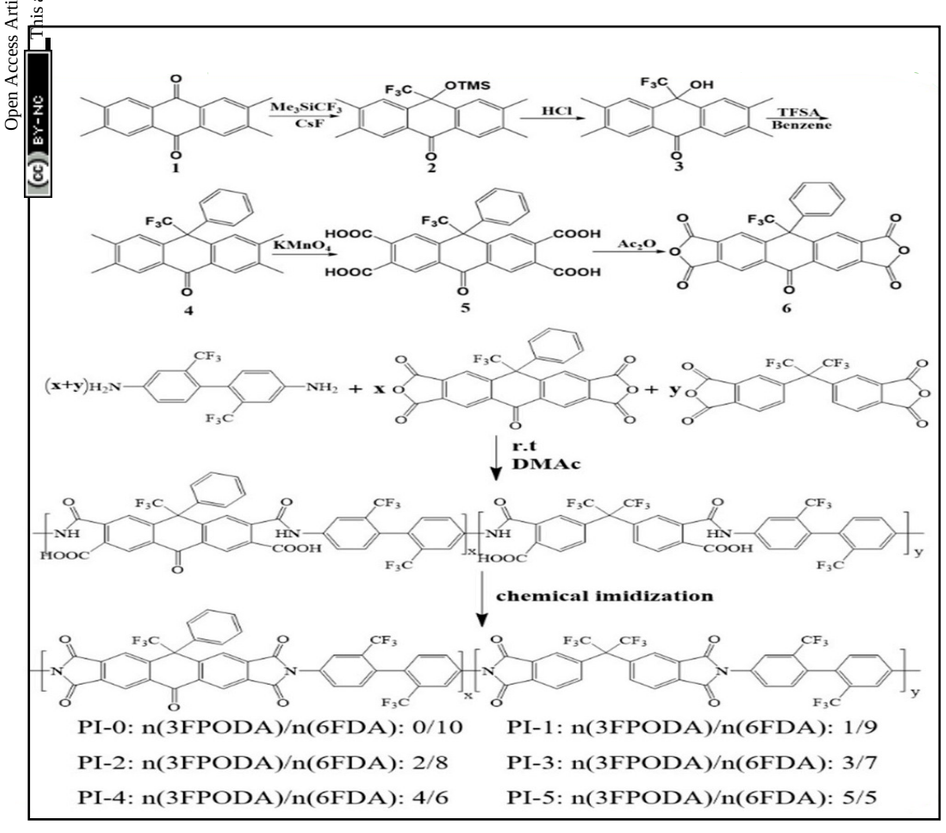

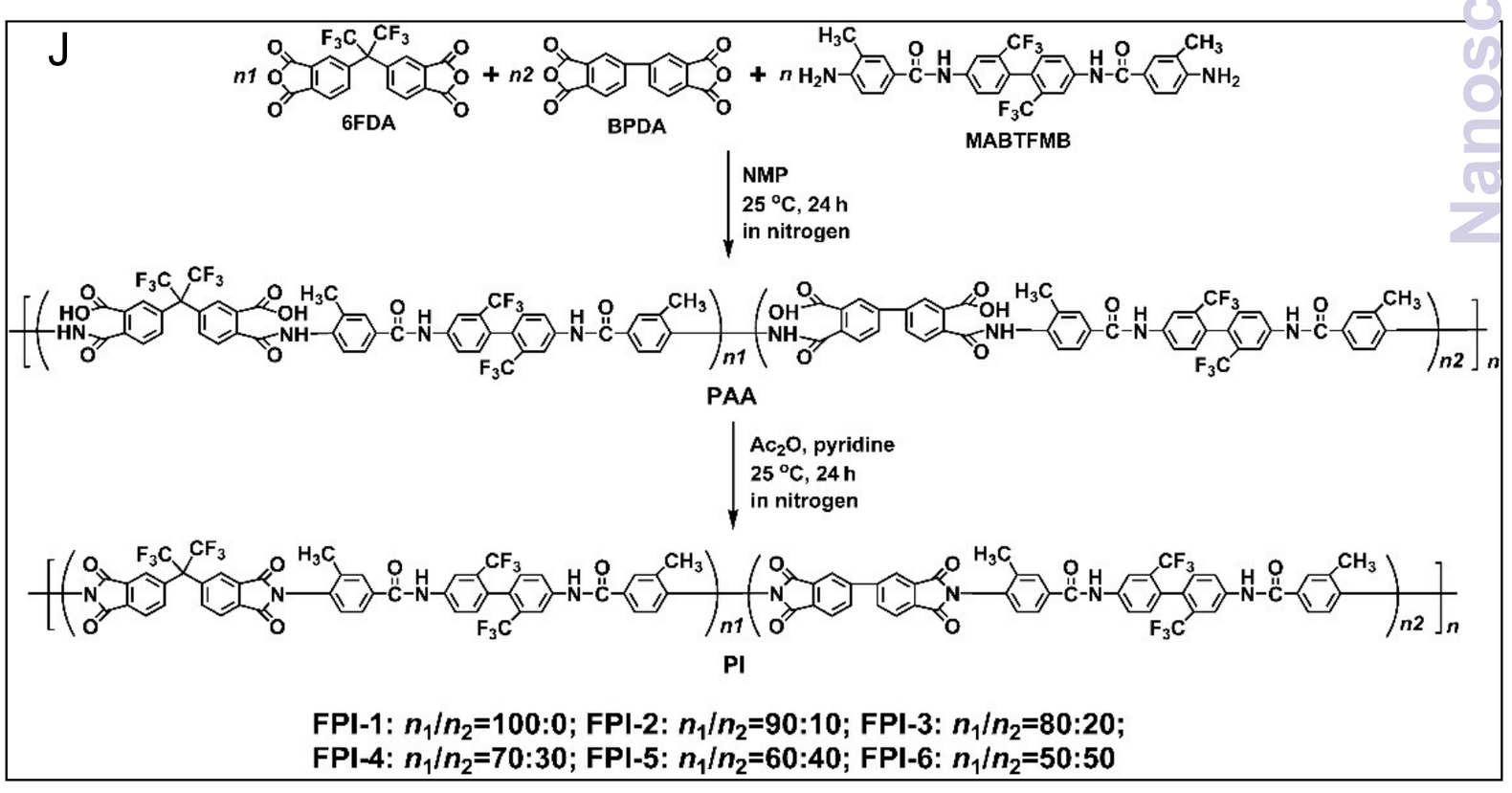

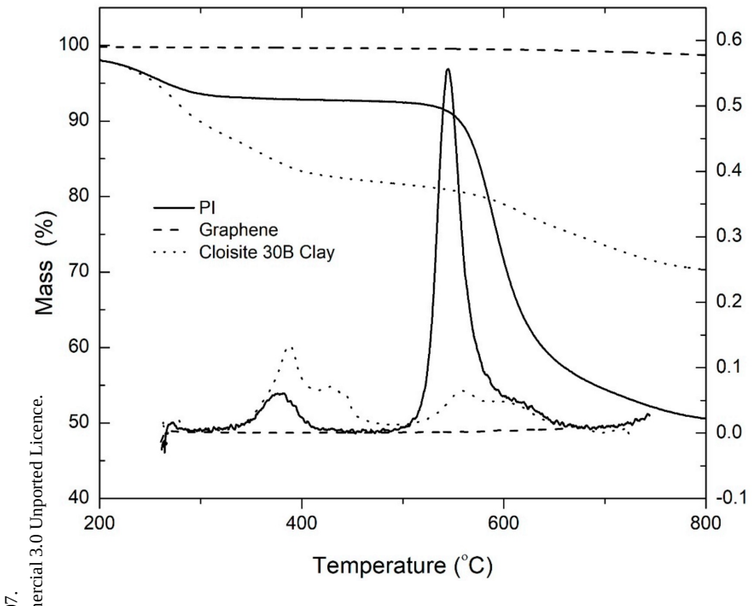

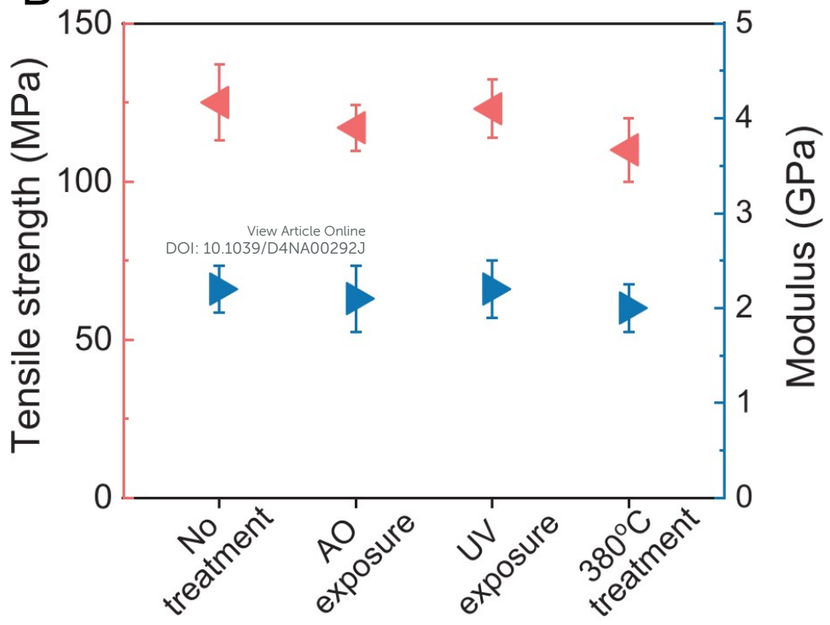

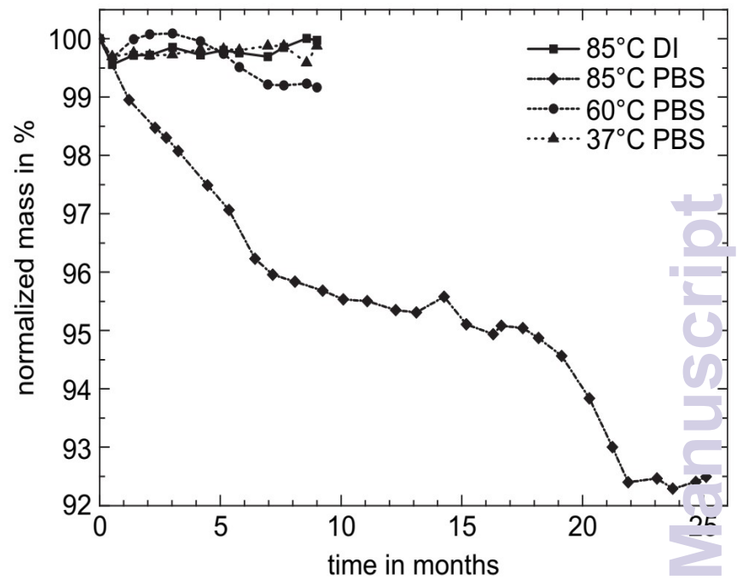

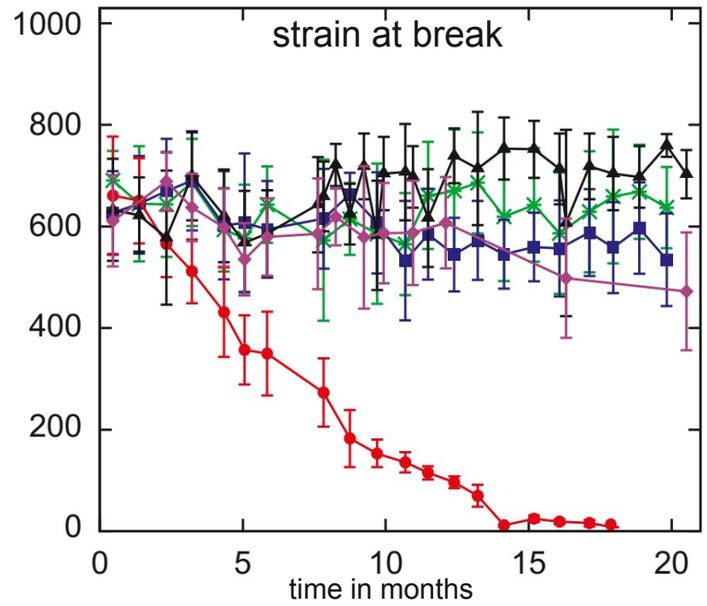

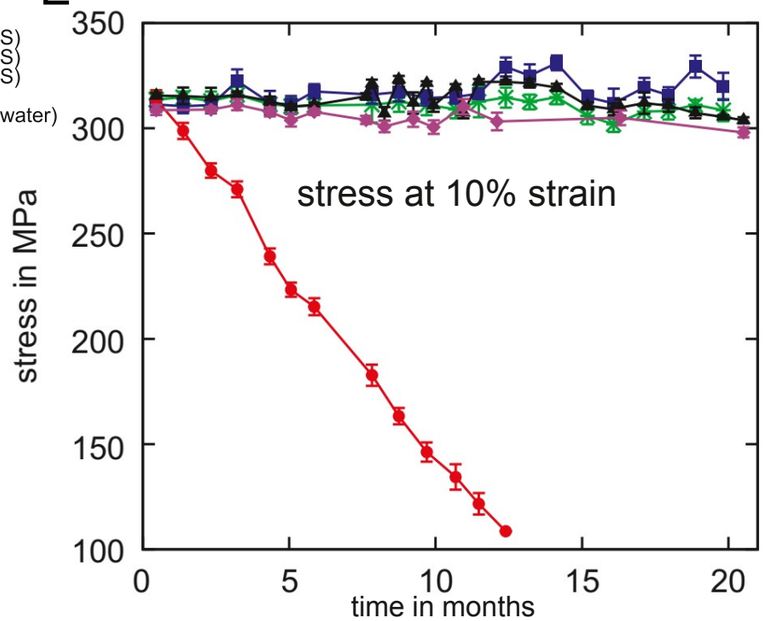

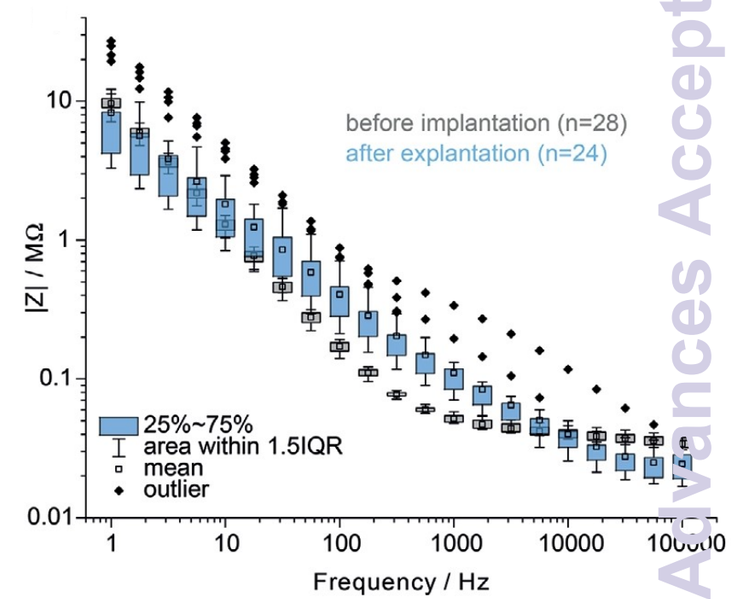

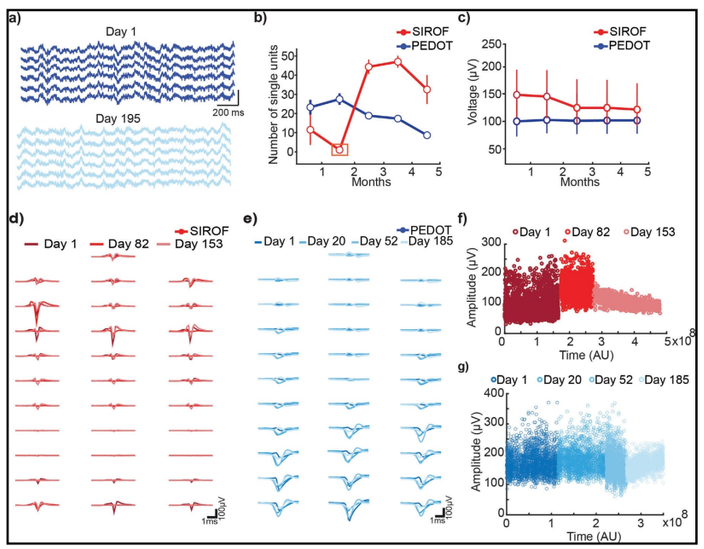

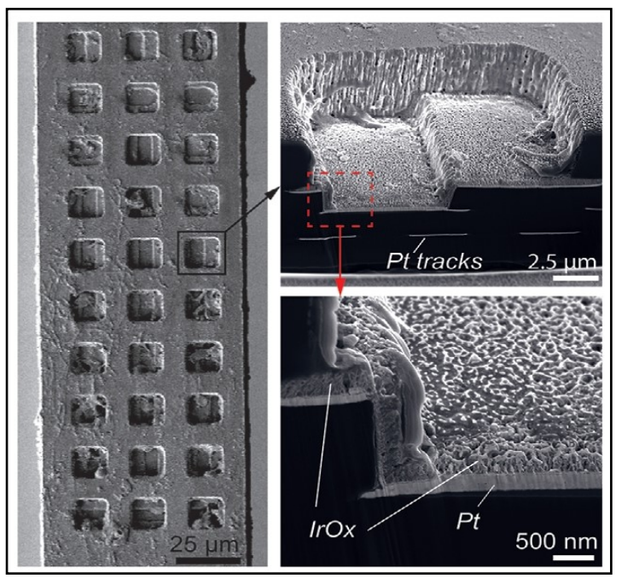

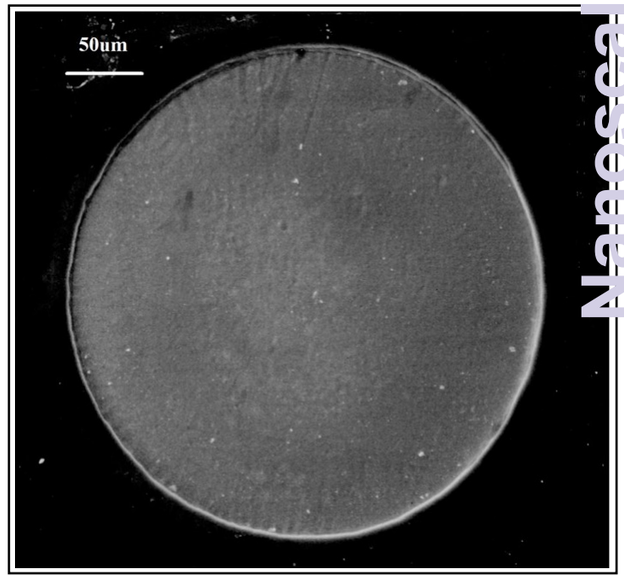

A

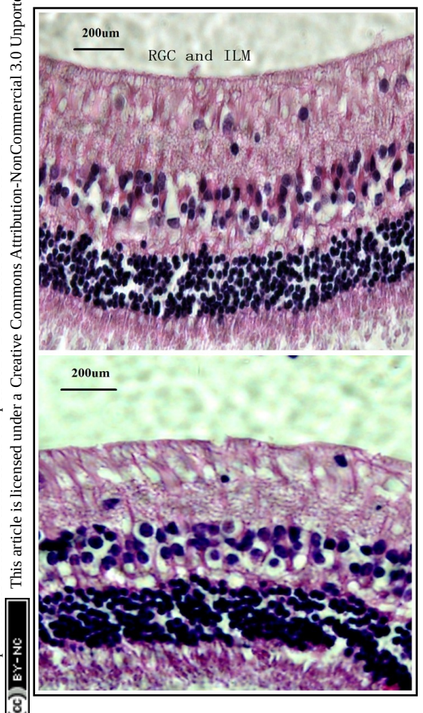

B

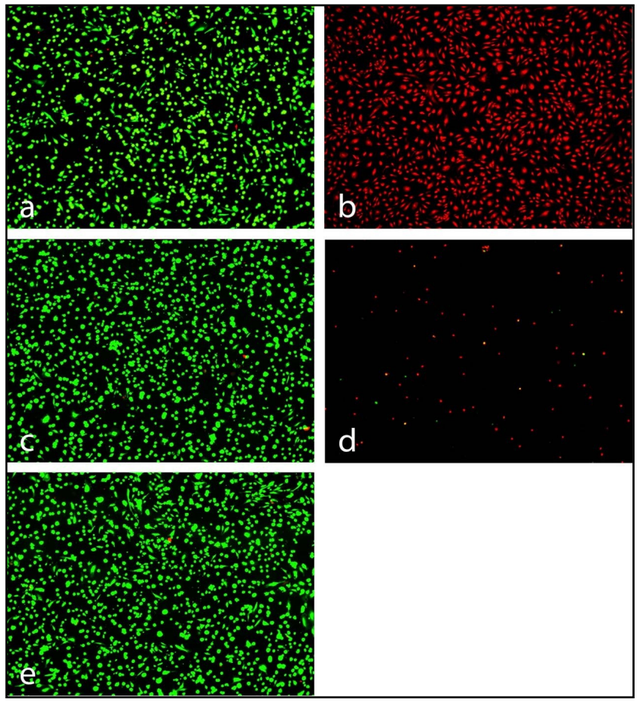

C

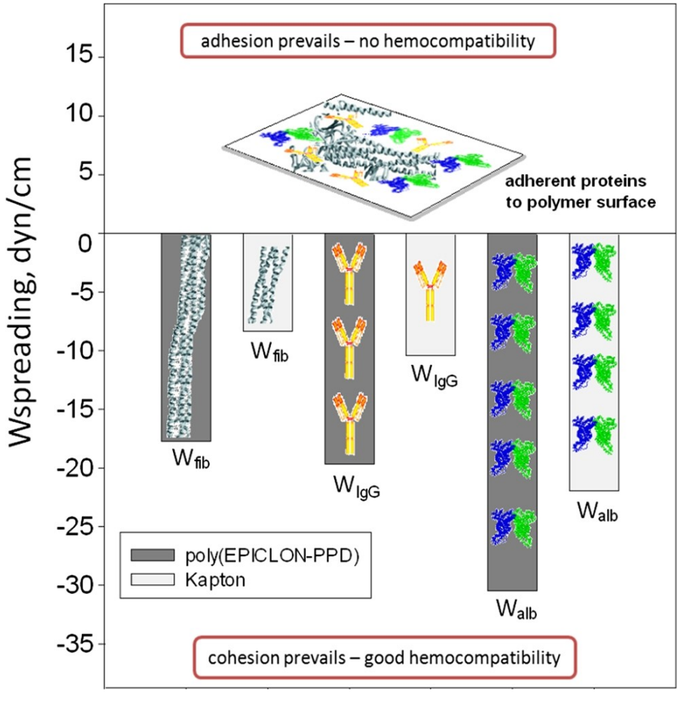

D

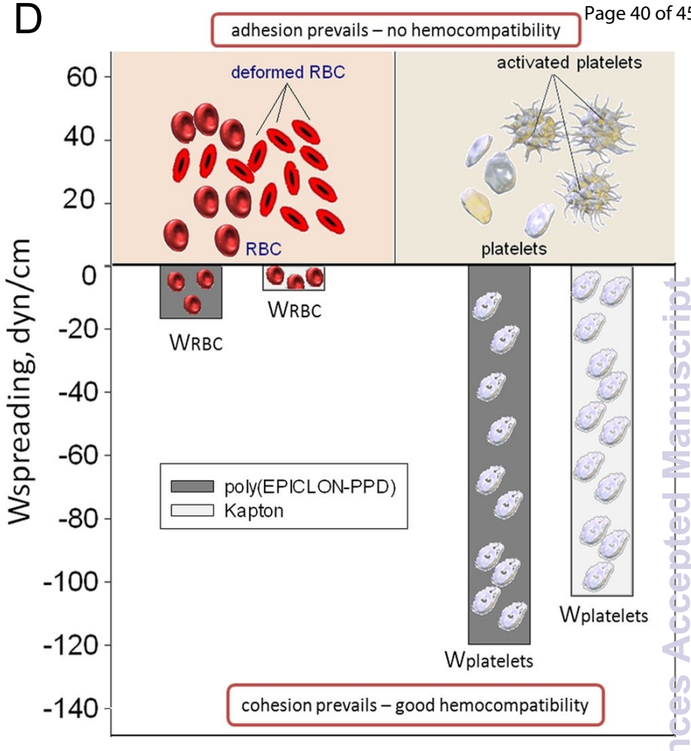

E

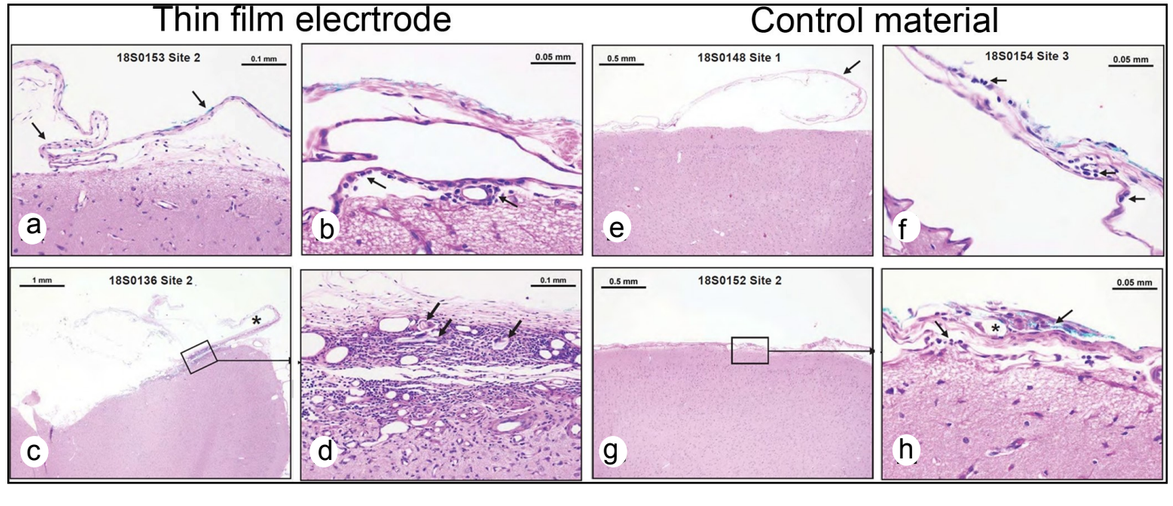

F

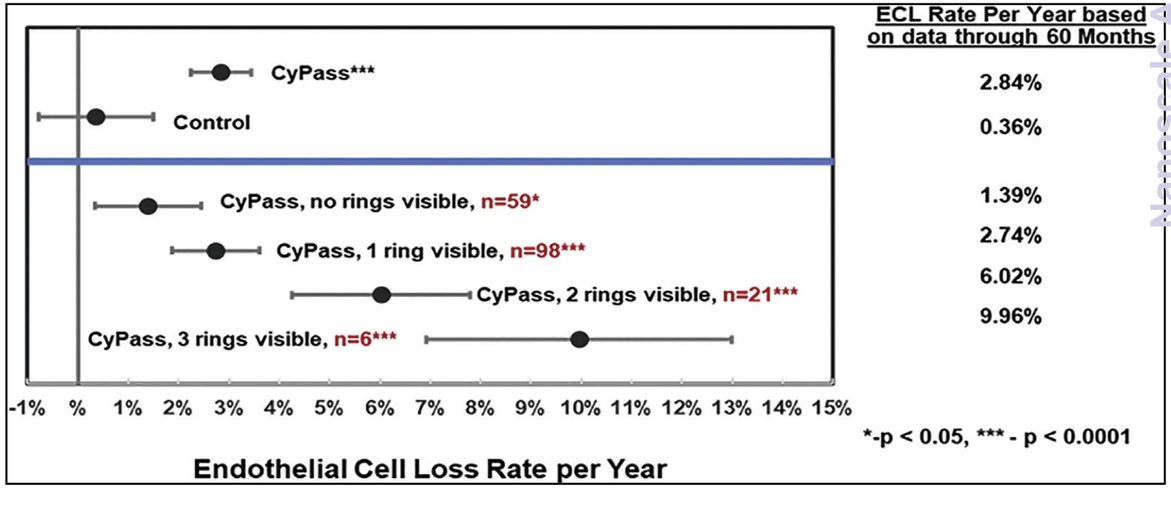

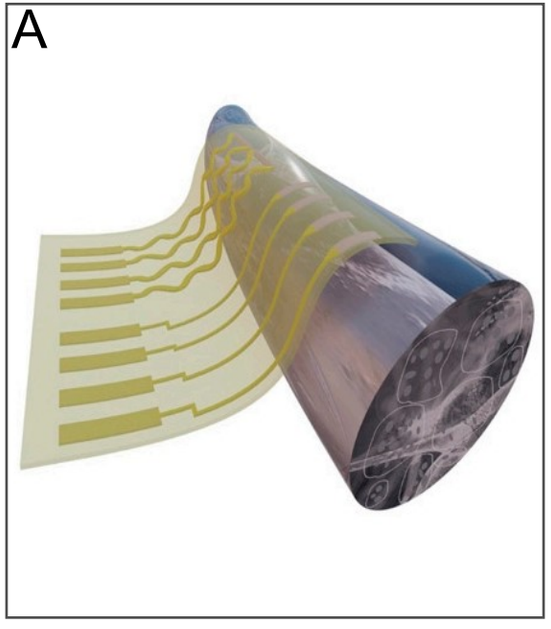

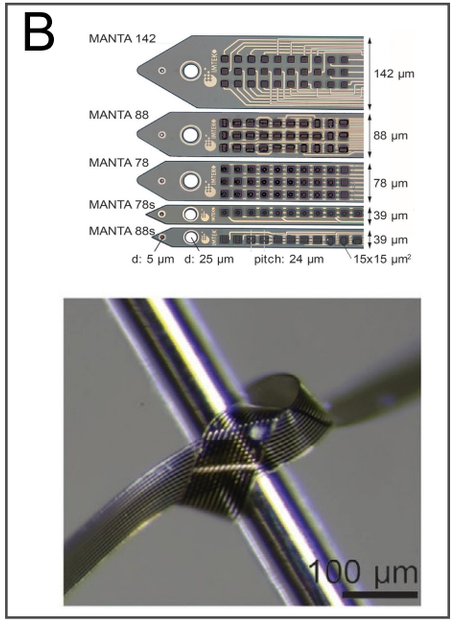

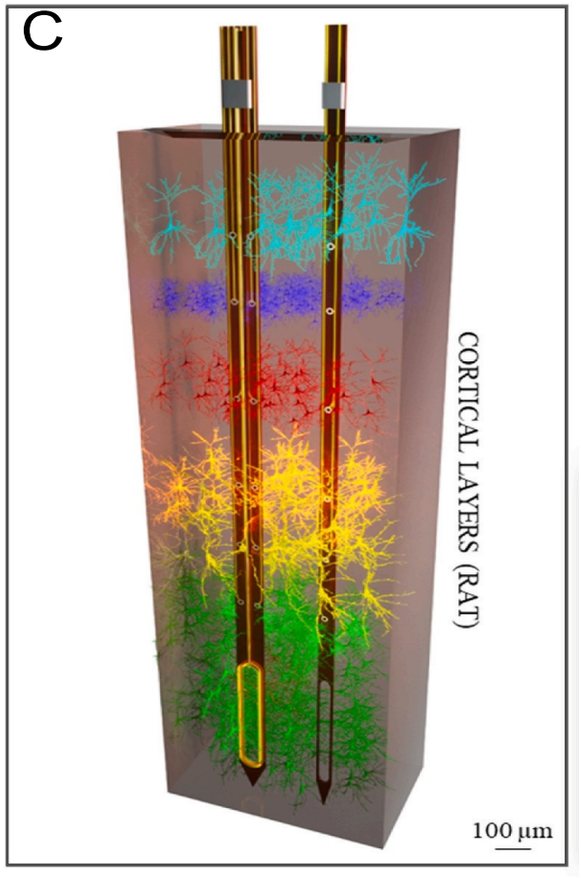

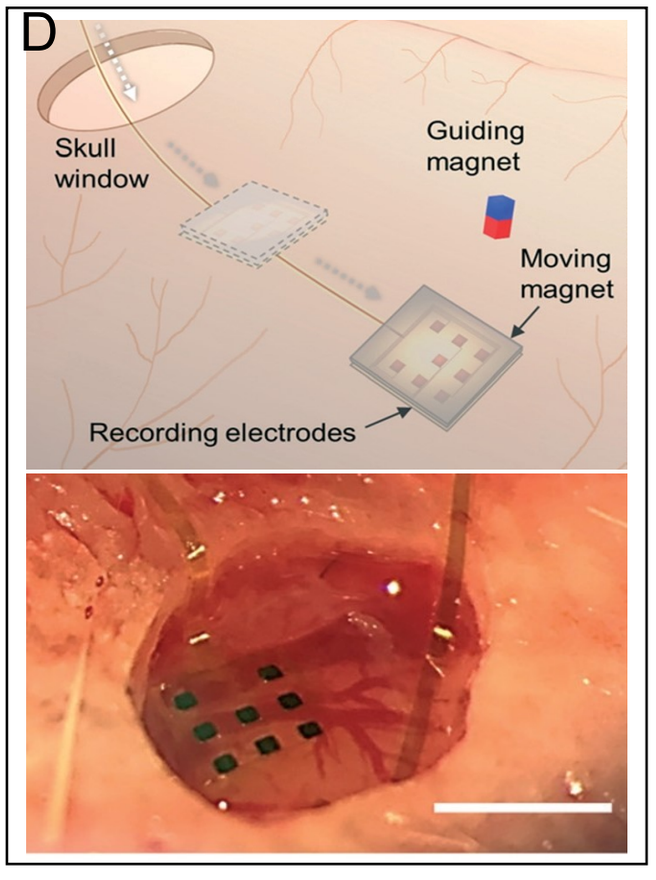

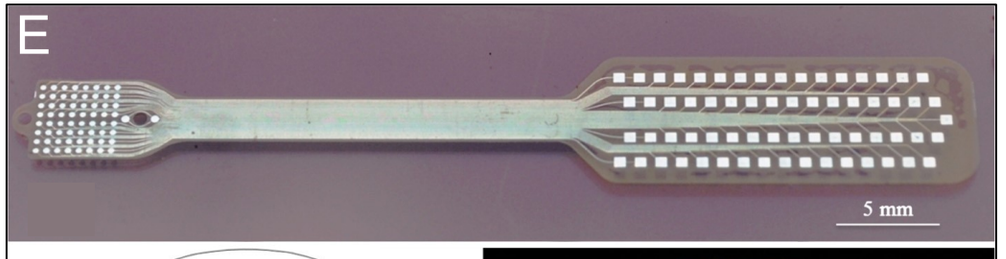

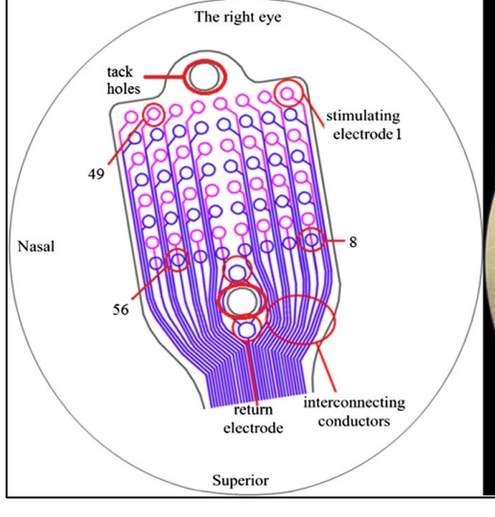

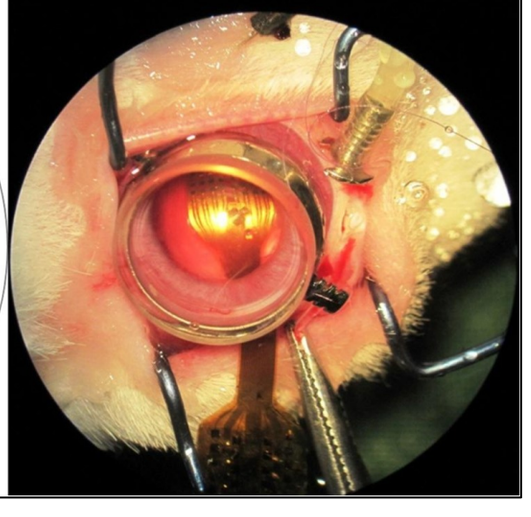

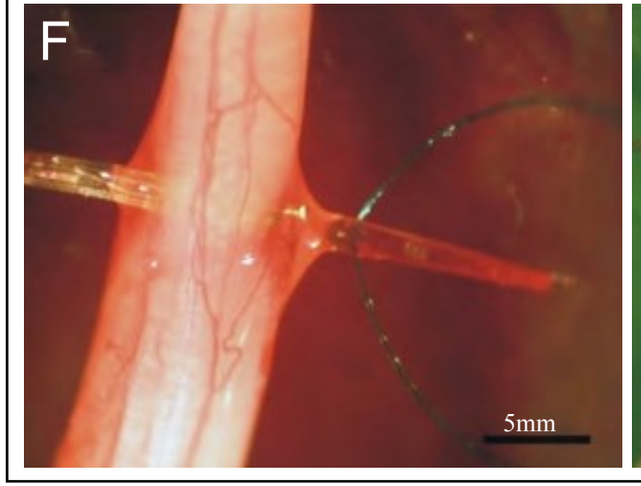

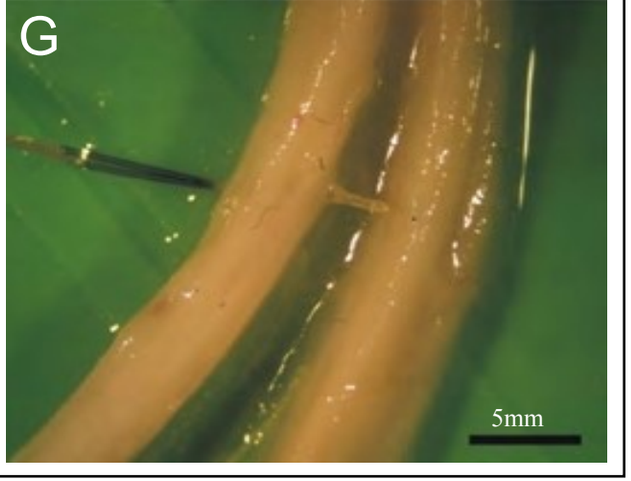

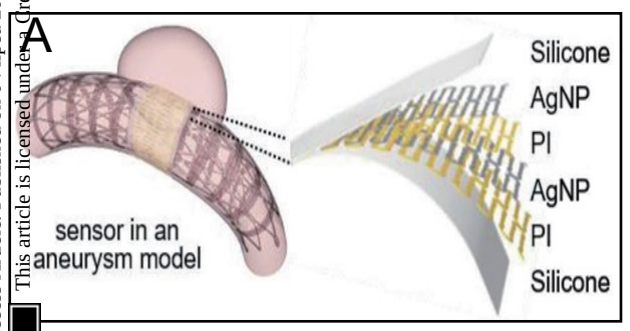

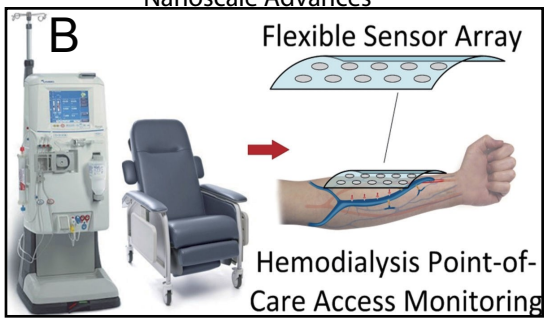

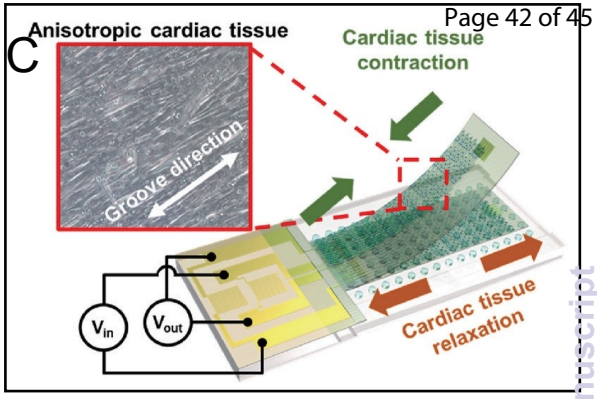

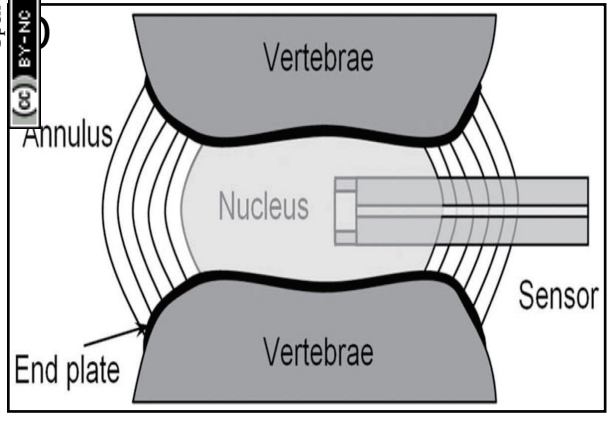

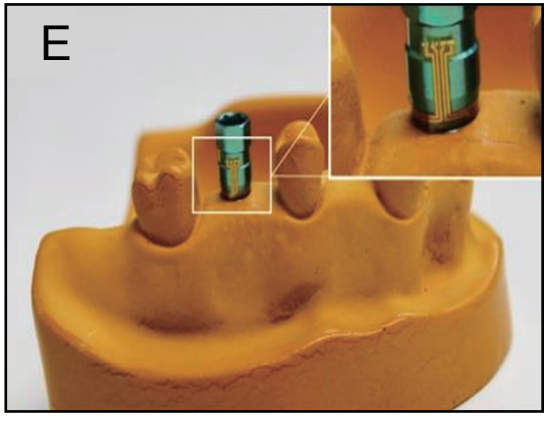

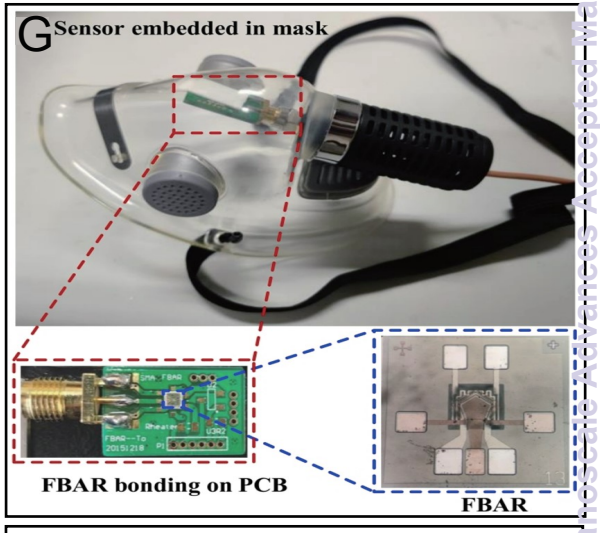

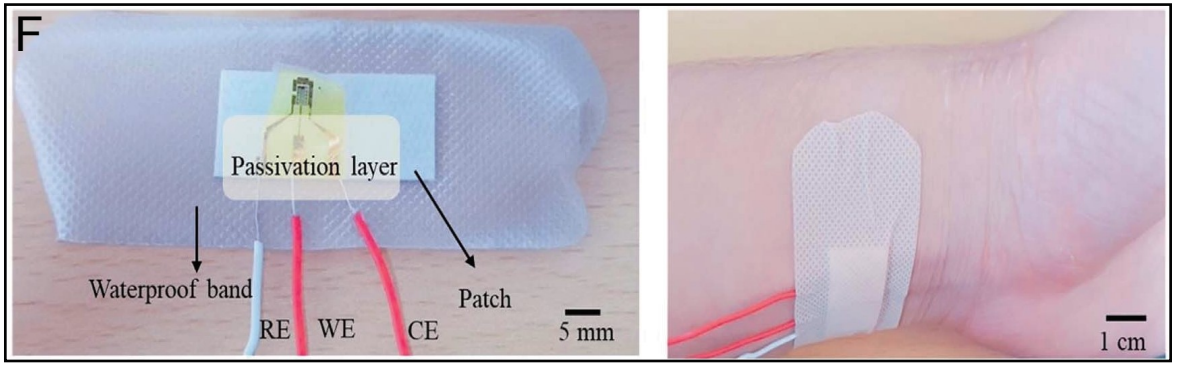

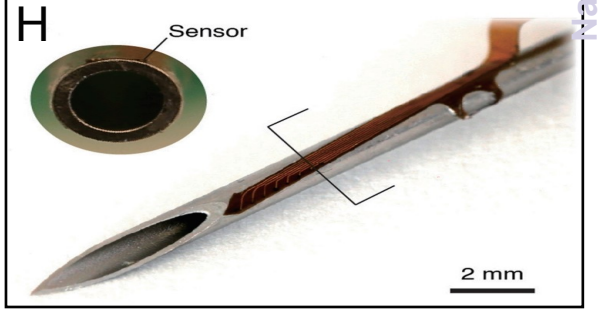

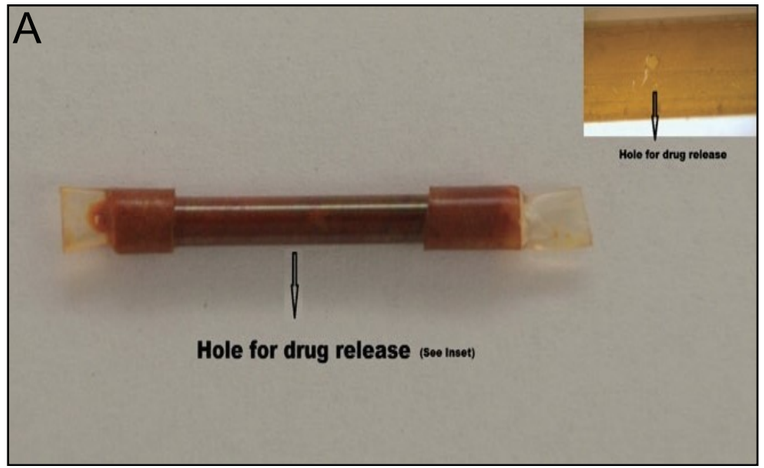

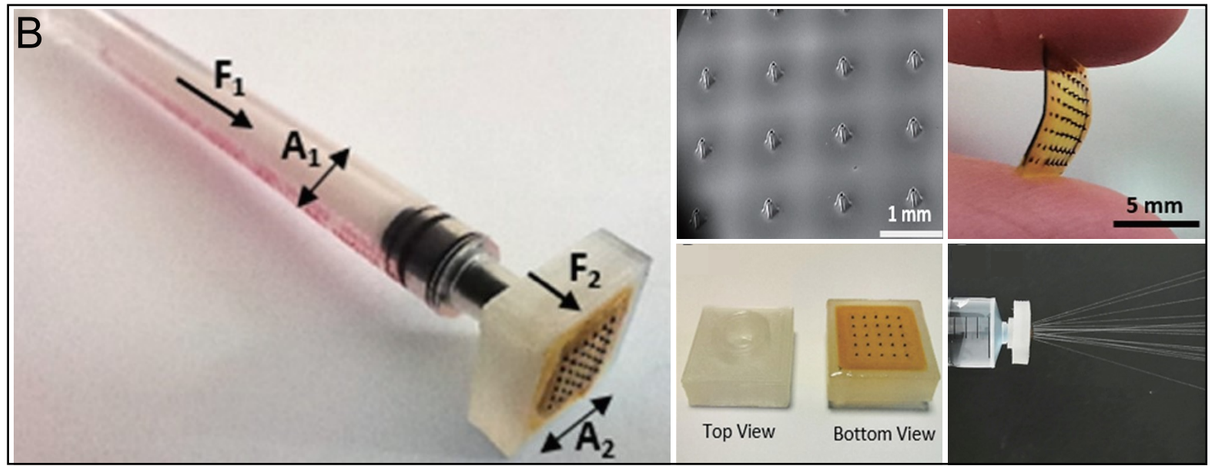

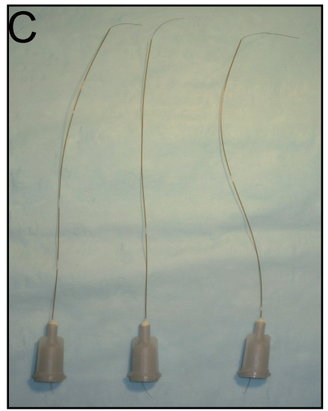

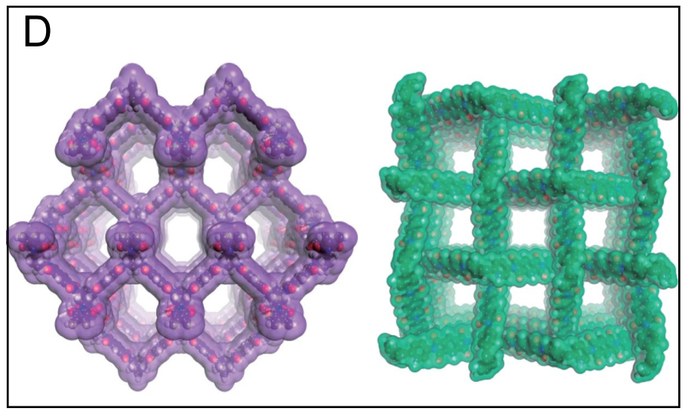

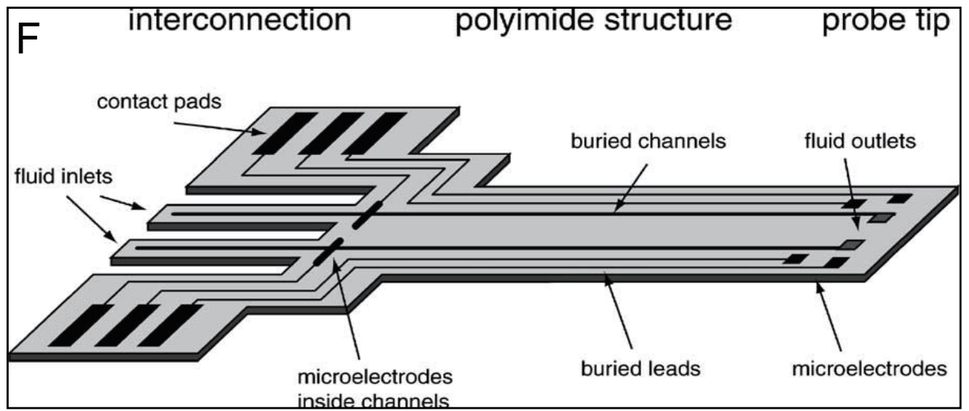

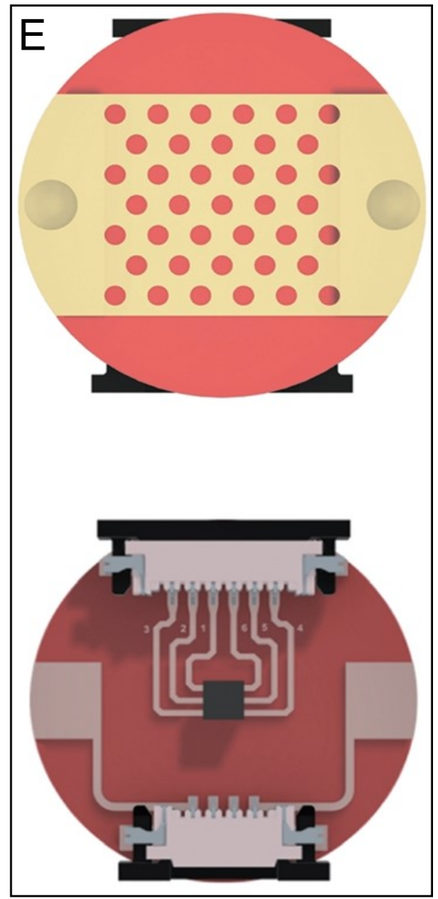

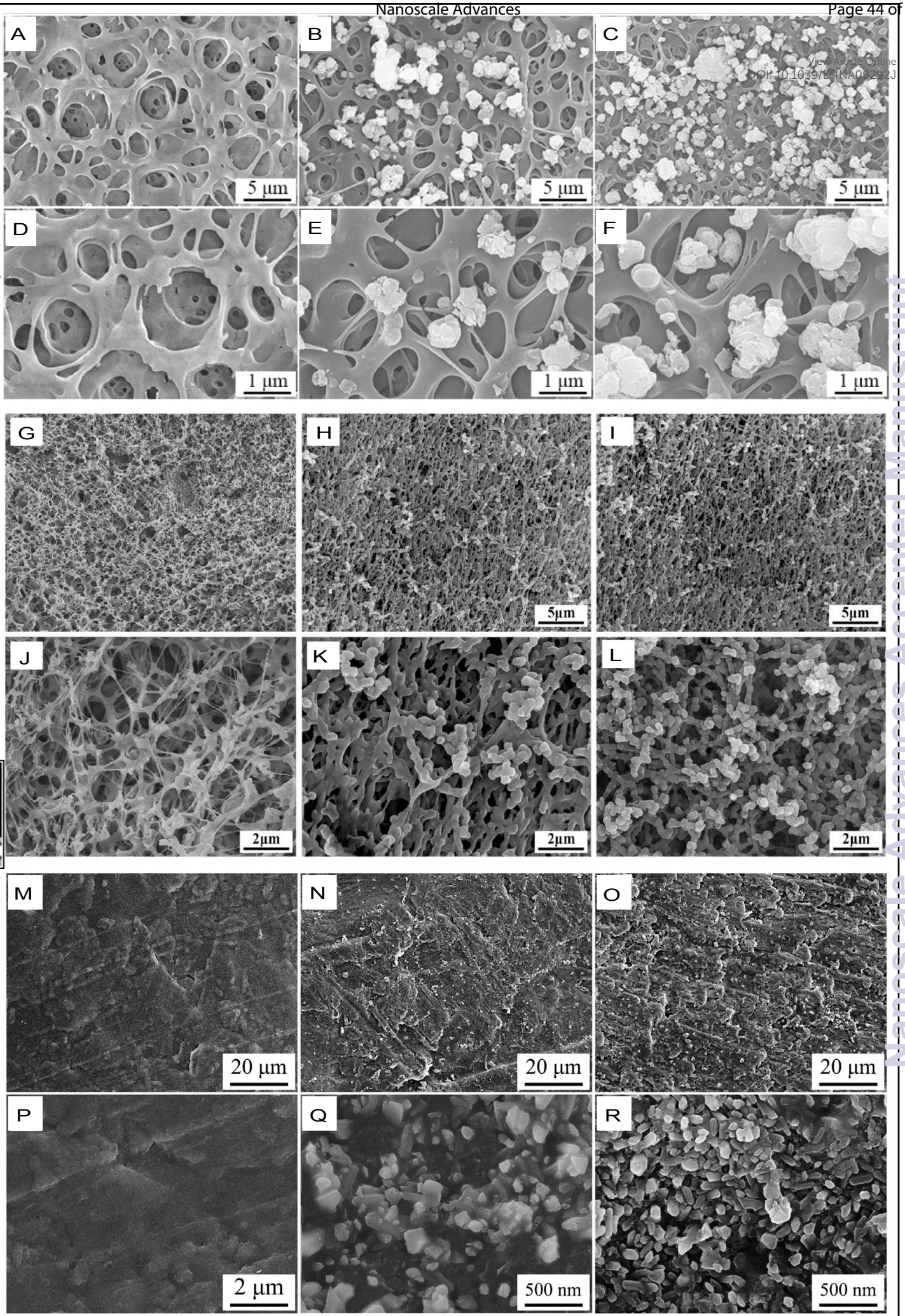

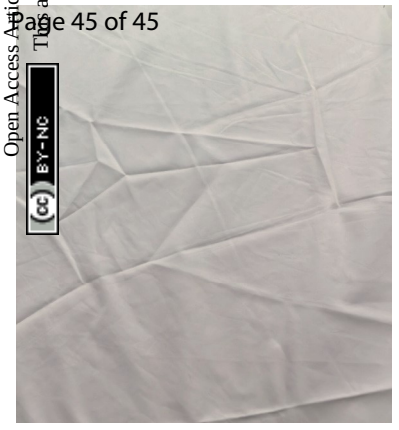

PI film 1

PI film 2

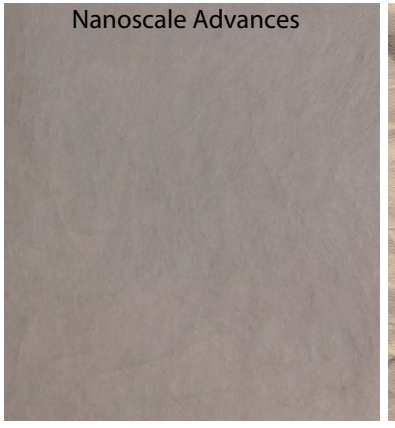

PI film 3

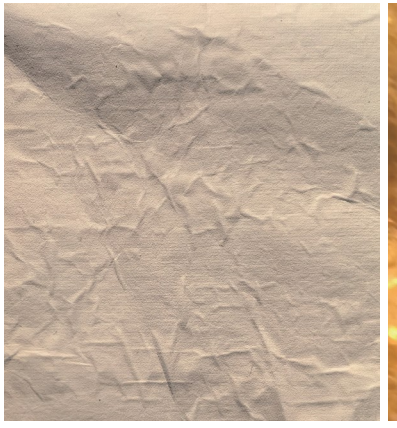

PI patch

PI fiber

PI fabrics 1

PI fabrics 2

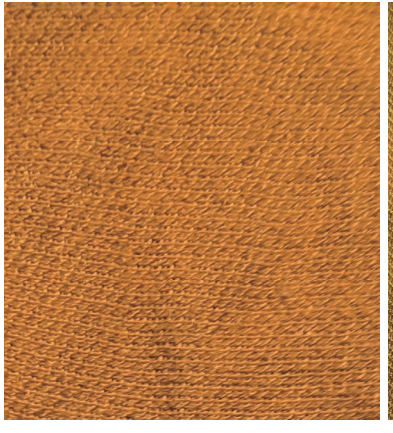

PI fabrics 3

PI fabrics 4

PI gauze